American Journal of Environmental Sciences

Review Article

Modeling the Nile: A Comprehensive Water Budget and Flow Assessment with the River Basin Flow Model (RBFM)

Youssef Ismail Hafez

Independent Researcher, Egypt

Article history
Received: 24-10-2024
Revised: 21-12-2024
Accepted: 06-01-2025

Abstract: The Nile River basin, covering 2.9 million km³ across 11 countries, is one of the world's most complex hydrological systems. With an annual historical discharge of 84 billion m³ at Aswan, Egypt, and rainfall of around 1,660 billion m³ per year over the Nile basin, effective management of this vital transboundary resource requires a deep understanding of its hydrology. This study offers a comprehensive description of the Nile's hydrology and presents a detailed review of the existing flow models applied to the basin. To advance this understanding, the study introduces a new water budget model, the River Basin Flow Model (RBFM), designed to simulate water dynamics across the entire Nile River basin. The RBFM divides the basin into interconnected units, where each unit is characterized by variables such as rainfall, evaporation, seepage, area, water depth, bed elevation, slope, and the number of connected catchments. For each connected catchment, the model incorporates factors such as area, rainfall, losses, and runoff coefficients. By simulating the water budget for each unit, the model calculates the resulting outflow. Although currently run on an annual basis due to data constraints, the model is capable of simulating monthly or finer temporal steps. The RBFM closely matches historical data, replicating the Nile's long-term average discharge: 24.1 billion m³ from the White Nile, 49.6 billion m³ from the Blue Nile, and 84.1 billion m³ at Lake Nasser, aligning with observed values from 1910-1995. The model also examines the impacts of changes in land cover, rainfall, and land use on the basin's water yield. It demonstrates that the Blue Nile is more sensitive to such changes compared to the White Nile, offering valuable insights into how environmental and anthropogenic factors affect the river's flow. This study underscores the RBFM's value as a simple yet effective tool for assessing the impacts of climate change, land use modifications, and dam construction on the Nile's water resources. Its minimal data requirements make it adaptable for application in other river basins globally. The model offers a practical approach for sustainable water management and policy development, supporting informed decision-making for one of the world's most critical river systems.

Keywords: Nile Basin, River Basin Modeling, Water Budget, Hydrology, Climate Change, Water Resources Management

Introduction

The Nile basin, as shown in Figs. (1-2), is one of the largest basins in the world, with a drainage area of approximately 2.9 million km² and a river length of around 6,500 km. The mean annual discharge at Aswan, the southern border of Egypt, is about 84 billion m³ and the annual sediment load at Aswan is estimated at 124 million tons per year (Abul-Atta, 1978).

The Nile basin extends from latitude 4° south to 31° north, spanning from central Africa to the Mediterranean Sea. Within this vast geographical area, the Nile basin includes a total lake area of 81,550 km² and swampy reaches amounting to 67,000 km² (Abul-Atta, 1978). The basin covers parts of eleven African countries: Burundi, Egypt, Eritrea, Ethiopia, Kenya, Rwanda, Sudan, South Sudan, Tanzania, Uganda and the Democratic Republic of Congo.

According to Abul-Atta (1978), the Nile has two "main" sources, the Equatorial lakes plateau and the Ethiopian plateau, although there are other sources that

DOI: 10.3844/ajessp.2025.49.78

contribute relatively less to the overall flow. The Nile basin is characterized by diverse climates, flora and fauna, as well as varying races, civilizations, languages, habits and religions across its vast spatial extent (Abul-Atta, 1978).

Corroborating the earlier findings, Mohamed et al. (2005) reported that the Nile basin covers an area of over 3 million km² and a length of about 6,700 km, making it the longest river in the world. The basin extends from 4° south to 32° north, encompassing various geographical, climatological and topographical regions. Precipitation in the basin generally increases southward and with increasing altitude, with virtually no rainfall in the Sahara desert and up to 1,200-1,600 mm/year on the Ethiopian and Equatorial lakes plateaus. The atmospheric moisture over the Nile basin is supplied by the Atlantic and Indian Oceans (Mohamed et al., 2005).

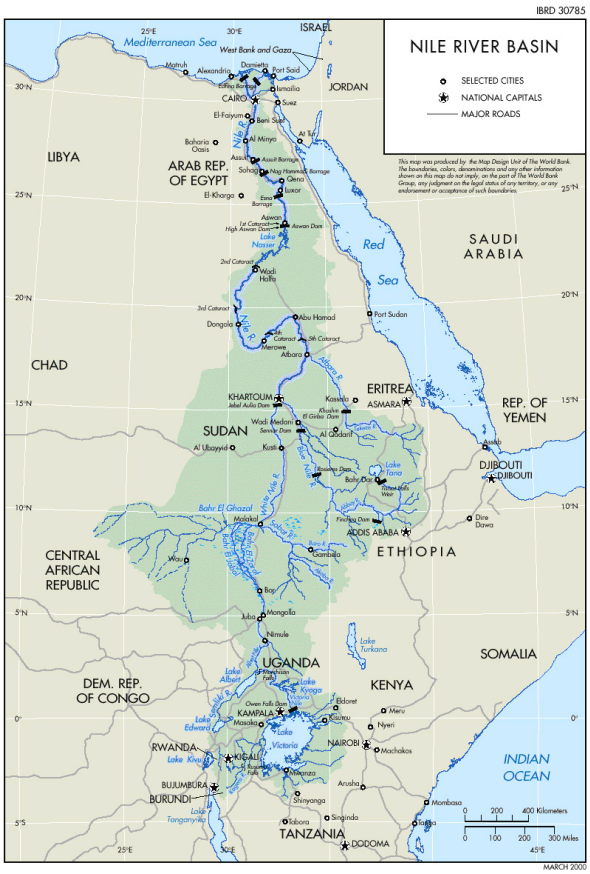

Fig. 1: Map of the Nile Basin in March 2000, source: World Bank and *https://historicaleve.com/map-with-nile-river/*

The Blue Nile is the main tributary of the Nile River, contributing the largest flow among all major tributaries, discharging about 50 Billion cubic meters/year (BCM/y) on average: However, the annual flow of the Blue Nile has shown significant variability, ranging from 2069 BCM/y in 1913 to 6985 BCM/y in 1929 (AbuZeid, 2019) The other major Nile tributaries include the White Nile (285 BCM/y), the Atbara River (12 BCM/y) and the Rahad and Dinder Rivers (4 BCM/y) at Khartoum The historical 10-year average flows of the Blue Nile have been estimated at 38 BCM/year (lowest), 45 BCM/year (moderate) and 50 BCM/year (average) (AbuZeid, 2019).

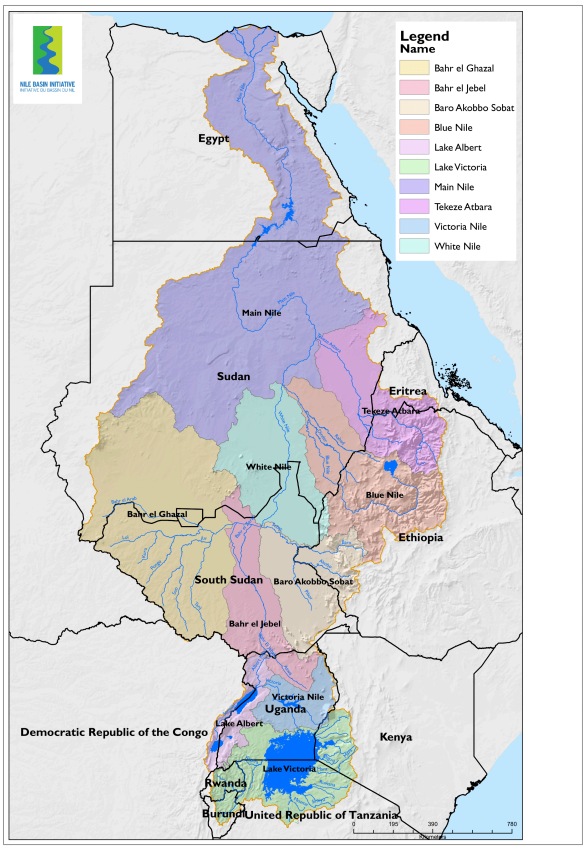

Fig. 2: Map of the Nile Basin, source Nile Basin Initiative and https//historicaleve.com/map-with-nile-river/

Effective management of the Nile basin requires a thorough understanding of the interactions between hydrological conditions, climatic conditions, land use and cover and human activities, particularly the upstream-downstream dynamics. To this end, a hydrologic model called the River Basin Flow Model (RBFM) has been developed to calculate the Nile flows from the equatorial lakes in the south to the Blue Nile Basin in the east and down to Lake Nasser in Egypt in the north.

Materials and Methods

Description of the Study Area and Data

The following information about description of the Nile Hydrology in its natural state as of the 1970's is taken from Abul-Atta (1978) which more or less represents the basin conditions before extensive

DOI: 10.3844/ajessp.2025.49.78

damming projects in the 21st century. Figure (3) shows the various hydrological units of the Nile basin which approximates the complex network of streams and lakes comprising the complex Nile basin in Figs. (1-2). It should be noted that the description given here about the Nile basin hydrology and its connecting water bodies is rare to find elsewhere. Most publications on the Nile basin present brief description of the Nile basin with focus mainly on the modeling aspects.

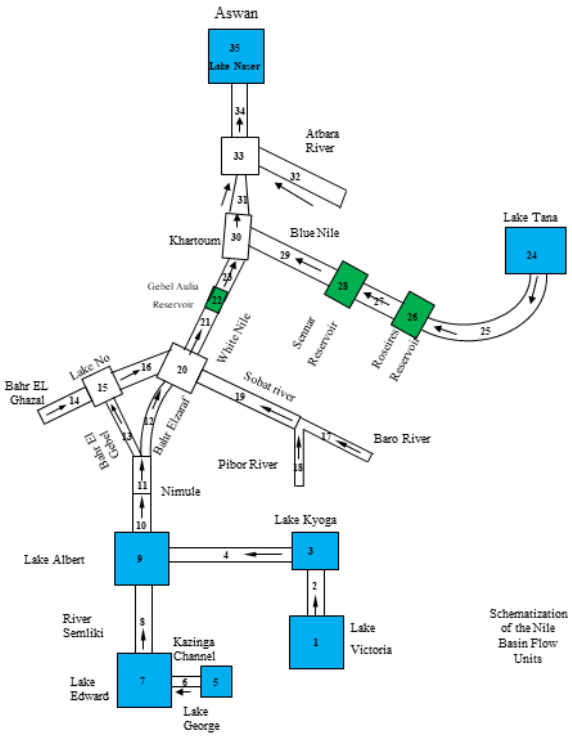

Fig. 3: Nile Basin model with 35 units (based on Abul-Atta, 1978 schematization) [Nile Basin model with 35 units]

Sources of Yield from the Equatorial Lakes Plateau

Lake Victoria

Lake Victoria has an area of 67,000 km³ and a surface level of 1,132.6 m above sea level. The rainfall catchment basin that feeds the lake covers an area of 195,000 km³.

The annual rainfall rate on the lake is 1.50 m per year. This means the direct annual rainfall on the lake is approximately 1.5 * 67,000 = 100,000 million m³ or 100 Billion m³ (BCM).

The annual rainfall on the catchment area around the lake is 1.15 m. About 8% of this rainfall flows into the lake, while the remaining 92% is lost to evaporation or infiltration. The net annual inflow to the lake from this source is around 195,000 * 1.5* 0.08 = 18,000 million m³ or 18 BCM.

The total annual water inflow to the lake is therefore approximately 118,000 million m³ (118 BCM).

Studies show the lake's evaporation rate is 1.26 m per year. This means the lake's annual loss through evaporation is around 1.26 * 67,000 ≈ 84,500 million m³ (18.5 BCM). Abu El-Atta (1978) reports the annual net water yield of Lake Victoria is 23.5 BCM where it can be inferred that there is about 10 BCM of another losses which might be due to seepage through the lakes bed floor. This amount of seepage represents seepage rate of about 0.1493 m/year over the 67,000 km³ area of the lake. In conclusion the net annual yield is =118 - 84.5 – 10 = 23.5 BCM.

Victoria Nile between Lake Victoria and Lake Kyoga:

The Victoria Nile is the only outlet from Lake Victoria, with the water flowing over several waterfalls, including the Ripon Falls and the Owen Falls near Jinja, Uganda.

The average drop over these falls is about 20 m. In the 1950s, Egypt and Uganda collaborated to construct the Owen Falls Dam to generate electricity for Uganda and also to enable storage in Lake Victoria as part of a larger project for the Equatorial lakes.

The Victoria Nile flows over successive waterfalls until it reaches Namasagali, 80 km from the outlet of Lake Victoria, where the river waters are discharged into Lake Kyoga.

The total drop in water level between Lake Victoria and Lake Kyoga is approximately 102 m.

Lake Kyoga

Lake Kyoga is a unique waterbody that differs significantly from Lake Victoria, characterized by its vast swampy surroundings. The lake itself covers an area of approximately 1,760 km², while the surrounding swamps span around 4,510 km². The catchment area of the Victoria Nile and Lake Kyoga is substantial, covering around 75,000 km². The region experiences an average annual rainfall of about 1.29 m.

Water Balance and Evaporation at Lake Kyoga

The total volume of annual rainfall over the lake and its surrounding swamps is approximately 8 billion cubic meters (6270×1.29 Million m³). In addition, rainfall on the catchment basin around the lake and its swamps amounts to 3 billion cubic meters per annum. Therefore, the total amount of water flowing into the lake and falling directly on it is around 11 billion cubic meters.

The annual evaporation rate from the lake surface is about 1.2 m, while it is 2.23 m from the swamps. Consequently, the total evaporation losses are approximately 12 billion cubic meters (1760×1.2+4510×2.23 Million m³).

Net Inflow and Outflow at Lake Kyoga

The net inflow to the lake itself and into the Victoria Nile, excluding Lake Victoria discharges, is -1.0 billion

DOI: 10.3844/ajessp.2025.49.78

cubic meters per annum (11-12). This suggests that Lake Kyoga is a source of water losses, estimated to be around -1.0 billion cubic meters per annum.

Considering the average annual discharge flowing into Lake Kyoga from Lake Victoria is 23.5 billion cubic meters, the average annual discharge flowing out of Lake Kyoga is approximately 22.5 billion cubic meters.

Victoria Nile: From Lake Kyoga to Lake Albert

The Victoria Nile flows naturally from Lake Kyoga, following a normal gradient for about 80 km until it reaches Kamdini. From this point, the water flows over waterfalls, culminating at Murchison Falls, around 100 kilometers from Kamdini.

The total drop between Lake Kyoga's water level at Massindi Port and the inlet of Lake Albert, downstream of Murchison Falls, is approximately 409 m.

Additionally, the total drop of the waterfall between Lake Victoria's water level (1132.6 m) and the water level at Fajao (618.8 m) is around 514 m.

Lake Albert:

- The average surface area of Lake Albert is 5,300 km²
- The Victoria Nile discharges its water into the northern end of the lake, while the Semliki River discharges its water into the southern end
- The Semliki River derives part of its water from rainfall in its own basin and the remainder from Lake Edward, which is connected to Lake George by the Kazinga Channel

Lake George:

- The surface area of Lake George is 300 km²
- The area of the lake's catchment basin is 8,000 km²
- The average lake level is 912 m above sea level

Lake Edward:

- The surface area of Lake Edward is 2,200 km²
- The area of the lake's catchment basin is 12,000 km²
- The average lake level is 912 m above sea level
- The average discharge from the lake's only outlet, the Semliki River, is about 2.5 billion m³ per year

The Semliki River:

- The area of the Semliki River basin is 8,000 km²
- The rate of rainfall in this basin is 1.7 m per year
- The volume of water flowing into the river from its basin (at a rate of 11%) is 1.5 billion m³ per year (8000×1.7×0.11 Million m³)
- The total discharge from the Semliki River into Lake Albert is 4.0 billion m³ per year (2.5 billion m³ from Lake Edward +1.5 billion m³ from the Semliki basin)

Lake Albert:

- The area of the Lake Albert basin is 17,000 km²
- The rate of rainfall on the basin is 1.256 m per year
- The volume of water flowing into the lake from its basin (at a rate of 12%) is 2.5 billion m³ per year (17,000 x 1.256 x 0.12 = 2,562 Million m³)
- The rate of rainfall on the surface of the lake is 0.71 m per year and the average surface area of this lake is 5,300 km³, resulting in a volume of 3.8 billion m³ per year (5,300 x 0.71 = 3,763 Million m³)
- The total volume of water flowing into Lake Albert is 32.8 billion m³ per year:
- From the Victoria Nile: 22.5 billion m³/year
- From the Semliki River: 4.0 billion m³/year
- From the lake basin: 2.5 billion m³/year
- Direct rainfall on the lake: 3.8 billion m³/year
- The sum of the above quantities is 32.8 billion m³/year
- Considering the lake's evaporation rate of 1.2 m per year (5,300 x 1.2 = 6,360 Million m³ = 6.3 billion m³/year), the net inflow of the lake is = 32.8 – 6.3 = 26.5 billion m³ per year

Albert Nile:

- The Albert Nile is the part of the Nile River that flows from the outlet of Lake Albert up to Nimule city, at the southern borders of Sudan (South Sudan now)
- From the outlet of the lake to Nimule, a distance of 225 km, the river flows at a gentle slope of approximately 2 cm per kilometer

Bahr El Gebel

From Nimule onwards, the river is known as Bahr El Gebel. Its waters flow over the Folla and Baiden waterfalls.

At the El-Rejaf gauge, located about 156 km from Nimule, the total drop over the waterfall is 155 m. Some tributary torrents discharge into Bahr El Gebel at this point, with an average annual volume estimated at Mongalla to be 4.8 billion m³. The average annual discharge from Lake Albert is estimated to be 26.5 billion m³ and the volume of water reaching Mongalla from this source is about 25.2 billion m³ per annum. The total average annual discharge at Mongalla is = 25.2 + 4.8 = 30 billion m³, which includes the torrential waters.

Beyond Mongalla, Bahr El Gebel crosses the Sudd region. Losses from the water passing by Mongalla are about 50%. The average flow to Malakal through Bahr El Zaraf and Bahr El Gebel courses totals 15 billion m³ per annum.

Bahr El Gebel in the Sudd Region

Dense growth of aquatic weeds (papyrus, Om Sufa, bamboo and hyacinth) begins to obstruct the river course north of Mongolla city on the river's right bank, forming large islands in the river itself and clustering over wide areas on either bank.

DOI: 10.3844/ajessp.2025.49.78

At the northern reach of Mongalla, the average water level drops from 440 m to 425 m at Tombe, that is 74 km from Mongalla, with an inclination of about 20 cm/km.

Swamps cover a wide area on the western side of the river, between Tombe and Bor, a distance of 67 km. This area is crossed by the Alyab river, which branches off to the left of Bahr El Gebel, north of Tombe, only to flow back into it again, at a point about 16 km away from Tombe.

North of Bor, the river course moves westwards, so that the swampy area now lies to the east and dry land to the west of the river.

At a distance of about 50 km north of Bor, Bahr El Gebel waters drain eastward through several inlets into a separate branch, known as the Atem river. This branch traverses the eastern swamps, until it gradually approaches dry land east of the swampy area. 80 km away from its point of origin, the Atem runs adjacent to the right side of Jonglei town and then flows towards Bahr El Gebel, into which it discharges through several outflows, the last of which is located about 200 km north of the point north of Jonglei.

Water drains from the lower extremities of the Atem River northwards, joining other tributaries from the right side of Bahr El Gebel itself, to form the Upper Zeraf. These waters, gradually increasing in quantity as they are supplemented by discharges from eastern Khors, constitute the main source of Bahr El Zeraf yield.

As for the left side of Bahr El Gebel, there are a number of subsidiary Khors to which water drains. The most important of these is Peak's Channel, which takes its water 325 km from Lake No, after which it flows back into Bahr El Gebel near El Zeraf, 295 km from Lake No.

The average surface area of the Bahr El Gebel swamps between latitude 5°, 15 and 9°, 30 is about 7200 km². The river here loses half of its yield through seepage, evaporation and transpiration.

Bahr El Ghazal Basin

The Bahr El Ghazal Basin is located in the southern part of Sudan, bordering the Republic of South Sudan and the Republic of Central Africa. The basin is characterized by the following key features.

Borders and Tributaries

To the south, the basin is bordered by the Sudan-Congo border, which contains the upstream reaches of the Tabari, Yei, El Na'am, Meridi, Tonj and Sueh (a main branch of the Jur River) rivers.

At the southwestern end, the basin is bordered by Sudan and the Central African Republic and is the source of the Busseri (a second branch of the Jur River), Pongo, Loll and southern tributaries of Bahr El Arab.

The northern part of the basin borders the southern slopes of the Mara Mountains, which contain the northern tributaries of Bahr El Arab.

Basin Characteristics

The Bahr El Ghazal Basin covers an estimated area of 526,000 km², with about 40,000 km² consisting of swamp zones.

The average annual rainfall in the basin is around 0.9 m, while the average annual evaporation rate is approximately 2.0 m.

Major Rivers

1. Bahr El Arab (basin area of 210,000 km²): Forms the northern half of the Bahr El Ghazal catchment, with its southern outlet flowing eastwards towards the Bahr El Ghazal swamps
2. Loll River (average annual discharge of 4.3 billion m³ at Nyamlell)
3. Pongo River (average annual discharge of 0.7 billion m³), the southern branch of the Loll River
4. Jur River (average annual discharge of 5.3 billion m³ at Wau): Considered the most important tributary in the area
5. Tonj River (average annual discharge of 1.1 billion m³)
6. Gel River (average annual discharge of 0.4 billion m³)

Water Discharge and Losses

The total average annual discharge from the six major rivers is estimated to be around 11.8 billion m³.

The El Na'am and Yei rivers, with estimated annual discharges of 0.5 and 2 billion m³ respectively, also flow towards Bahr El Gebel and lose their water in the swamps.

In total, the estimated average annual discharge from the Bahr El Ghazal basin tributaries is around 15.1 billion m³. However, most of this water is lost in the Bahr El Ghazal swamps, with only about 0.5 billion m³ per year reaching the White Nile.

Sources of Water Yield from the Ethiopian Plateau

El Sobat River

The El Sobat River emerges as a vital conduit of water contributing to the White Nile, showcasing a notable path of water flow and distribution that carries immense significance and unlocking potential.

The El Sobat River marks its journey with the convergence of significant branches. Notably, the Pibor River, a pivotal tributary, joins the main course of El Sobat, followed by the influential Baro River's integration downstream. This union of water bodies

DOI: 10.3844/ajessp.2025.49.78

enriches the flow dynamics, amplifying the river's strength.

The Baro River, coursing through the landscape with purpose, encounters challenges such as evaporation and seepage in swampy terrains. Despite such losses, the Baro branch brings a substantial annual discharge of 13.00 billion cubic meters at Gambeila, nurturing the combined flow towards the Sobat with 9.2 billion cubic meters annually.

Efforts to mitigate loss and optimize usage are imperative, especially in regions like Machar and associated khors, where water dissipates into swamps like the Machar swamps. Strategies for conservation and harnessing this lost water potential hold promise for enhancing overall water availability.

The Pibor River adds its share to the river's bounty, contributing around 2.8 billion cubic meters annually to the Sobat River's flow. The combined discharge from both branches accentuates the annual volume to an impressive 12.00 billion cubic meters, showcasing the river's robust capacity.

The journey towards the confluence of the two branches leads to a surge in volume, with the aggregate discharge escalating to 13.5 billion cubic meters annually at Hillet Doleib, where the Sobat River merges with the White Nile. This augmentation underscores the synergistic effect of seasonal variations and optimal water utilization.

A comprehensive view of the water landscape reveals a substantial annual average discharge at pivotal points like Malakal, emphasizing the collective contribution from Bahr El Gebel, El Zaraf, Bahr El Ghazal and the Sobat River, culminating in a total of 29.00 billion cubic meters per year. This abundance of water resources sustains ecosystems and livelihoods along the river's course.

As the river flows downstream, the cumulative yield translates to practical benefits, with a refined figure of 24 billion cubic meters per year at Aswan, accounting for normal losses along the river's path. This downstream impact underscores the interconnected nature of water systems and the significance of upstream conservation efforts for downstream utilization.

In essence, the El Sobat River emerges as a pivotal source of water yield from the Ethiopian Plateau, embodying a narrative of abundance, challenges and untapped potential. Harnessing the river's resources judiciously stands as a collective responsibility to ensure sustainable water management and unlock a prosperous future for the region's water landscapes.

The Blue Nile

The area of Lake Tana, the original source of the Blue Nile, is about 3,000 km³. The average level of its surface is 1,800 m above sea level. The discharge from Lake Tana into the Blue Nile is estimated at about 3.8 billion m³ per annum, about 940 km from El Rosaries.

The drop in water level from Lake Tana to El Rosaries is 1,310 m. Several other tributaries discharge into the Blue Nile, adding to the average river yield so that it reaches 50 billion m³ per annum at Rosaries, 270 km from Sennar reservoir. The drop in water level over this distance is 35 m. In the 390 km between Sennar and Khartoum, the tributaries of Dinder and Rahad join the Nile, flowing into it from the right, 215 km south of Khartoum. These tributaries add about 4 billion m³ per annum to the yield of the Blue Nile, so that its average total yield amounts to 54 billion m³ per annum. The river drop over this distance is 64 m.

The Blue Nile is a torrential river, violent in its flood season and capable of carrying fragmental rocks from the Ethiopian plateau. The formation of the Nile Delta is due to the silt carried by the Blue Nile and the Atbara River over thousands of years.

The average yield of the Blue Nile, estimated at Aswan and excluding normal losses, is about 48 billion m³ per annum.

River Atbara

The source of the Atbara River is in the Ethiopian mountains near Lake Tana, at a level of approximately 2,000 m. After flowing for 880 km, it joins the main Nile at Atbara city, 310 km to the north of Khartoum. Its slope and velocity exceed those of the Blue Nile, as its drop from its source to its outflow amounts to about 1,640 m. The most important of the Atbara branches is River Stit, which discharges into the Atbara about 510 km away from the latter's outflow into the main Nile. The average total discharge of the Atbara River is 12 billion m³ per annum, estimated at about 11.5 billion m³ at Aswan.

The Main Nile

Once the Blue Nile joins the White Nile at Khartoum, the river is known as the main Nile, up to its outflow into the Mediterranean in a journey 3,065 km long. Between Khartoum and Aswan, the river is 1,885 km long and crosses six waterfalls. The drop in water level over this distance amounts to about 200 m, based on the current storage at the High Dam.

The distance between Aswan and the Delta Barrages is 946 km. The average slope of the river is 1:13,000 and its average cross-sectional width is 900 m, with a cross sectional area of 5,700 m³.

Egypt had previously constructed the Old Aswan Dam for annual storage, as well as Esna, Hamadi, Assiut and Delta Barrages on this part of the Nile. At the Delta Barrages, the Nile bifurcates into the Damietta and Rosetta branches, each about 235 km long up to their outflow into the Mediterranean. Other constructions

DOI: 10.3844/ajessp.2025.49.78

include the Edfina Barrages on the Rosetta branch and the Zifta Barrages at Damietta, as well as an earth dam at Farascour, to be replaced by a permanent dam with a lock and a spillway on the eastern side, to facilitate navigation between Cairo and the Mediterranean Sea.

The annual average total of the normal Nile yield estimated at Aswan, from its various sources, is about 84 billion m³. The Blue Nile represents the largest tributary to the Main Nile providing an average annual flow of about 50 Billion Cubic Meters (BCM)) which is about 60% (50/84 = 0.595 ~ 0.6 = 60%) of the natural average flow of the Main Nile at Aswan in Egypt, AbuZeid (2019).

The Upper Blue Nile basin represents up to 60 % of the Ethiopian highlands' contribution to the Nile River flow, which is itself 85 % of the total (Abu-Zeid and Biswas, 1996; Conway, 2000). The area of the river basin enclosed by a section at the Ethiopia–Sudan border is about 175 315 km³, covering about 17 % of the total area of Ethiopia, Abera et al. (2017).

Fig. 4: Map of Eastern Nile region, with reservoir locations, after Wheeler et al. (2016)

Infrastructure

The major infrastructures on the Nile River basin include the following: the Low Aswan Dam, 1902 in Egypt, Sennar Dam, 1925, Jebel Aulia Dam, 1937, the Khashim El Girba Dam, 1964, Rosaries Dam, 1966, High Aswan Dam (HAD, 1970), Tekeze Dam, 2009 and Merowe Dam, 2009, Figure (4), Wheeler et al. (2016). Recently Ethiopia started the construction of the Grand Ethiopian Renaissance Dam (GERD, construction started on 2011 and as of July 2024 is currently going). GERD has a planned full supply elevation of 640 m and will create 74 BCM of reservoir storage – approximately 1.5 times the average annual flow at the dam location, Wheeler et al. (2016).

This investigation tries to present the hydrological modeling of the Nile basin to understand the dynamics and intricate connections between the various flow units based merely on science and scientific methods without adhering to any political position or stance. The following section introduces the most relevant works about modeling water flow in the Nile Basin followed by presenting the proposed River Basin Flow Model (RBFM) and lastly presenting its application to the Nile Basin.

Existing Modeling Work on the Nile Basin

Existing model studies of the Nile basin can be classified into four major categories as: (1) Flow simulation models (Conway, 1997; Mohamed et al., 2005; Abdel-Aziz, 2014; Abera et al., 2017; Abd-El Moneim et al., 2017; Belete et al., 2018; Kamel et al., 2019a) which could be further divied into water budget models (flow blance models) versus physically based distributed models, (2) Operational models for optimizing dams' operations and management, hydropower generation and reservoirs operations (Wheeler at al., 2016), (3) GERD hydrological and hydropower effects on the downstream countries (Digna et al., 2018; AbuZeid, 2019; 2021; Kamel et al., 2019b; Heggy et al., 2021; Hassan et al., 2023; Ahmed et al., 2024) and (4) GERD Dam Break scenarios (Mahmoud et al., 2022; Eldeeb et al., 2023) which focused mainly on GERD dam break collapse problems with its consequences on the downstream regions.

Most existing models dealing with the Nile focused on the Eastern Nile Basin (ENB) such as by Conway (1997) and increased significantly after the inception of controversial GERD (Wheeler, 2012; Abdel-Aziz, 2014; Abera et al., 2017; Abd-El Moneim et al., 2017; Kamel et al., 2019a) while others dealt with the whole basin (Mohamed et al., 2005; Belete et al., 2018). Almost all of these works represented their model structure and the modeling results. The focus primarily was to show the match between measured and simulated flows. This is done without presenting clear details about the dynamics and connectivity between the various Nile Basin hydrological flow units assuming familiarity of the readers with the dynamics and intricacy of the Nile Basin. A description of the most relevant work on modeling of the flows in the Nile River Basin is presented. The intention is not to give an exclusive and inclusive description of the all the modeling works on The Nile but rather to focus on those studies which are relevant to this stduy.

The use of physically-based (conceptual) water balance models is perhaps the most appropriate method for simulating the Nile River Basin flow. The problems involved with developing even the simplest models lie primarily in data availability. Concerning the Blue Nile Basin for example, most established hydrological models are data intensive, yet the Blue Nile has limited rain

gauge coverage, few long term temperature records, few gauged sub-catchments and very scarce daily data. The size and complexity of the Blue Nile, together with the lack of data, is therefore a severe constraint to the application of sophisticated hydrological model, Conway (1997). Conway (1997) describes the development and validation of a water balance model for the Upper Blue Nile basin in Ethiopia. Due to the limited availability of climate and hydrological data in this large river basin, the model uses a grid-based approach that requires relatively few data inputs and parameters. The model estimates Potential Evapotranspiration (PE) and rainfall for 10-minute grid cells based on multiple regression models using latitude, longitude and elevation.

The model by Conway (1997) is calibrated to reproduce mean monthly runoff over a 37-year period (1951-1987) as in Figure (5) and validated by its ability to simulate sub-catchment runoff and historical variations in Blue Nile runoff as in Table (1). The quality of rainfall inputs is the key factor determining model performance, with the best results obtained using long, high-quality station data. Over a 76-year period, Table (1), the correlation between observed and simulated annual flows was 0.74 and the mean error was 14%, although there were larger errors in individual years. Given the data limitations, these results are considered encouraging. Conway (1997) achieved a remarkable level of agreement between the 1951-1987 simulated and observed (across various periods) mean monthly runoff data during the calibration period for the entire Upper Blue Nile region as seen in Figure (5). Figure (5) revealed a consistent monthly discharge less than 1.0 billion cubic meters (BCM) until June, followed by a rapid, nearly linear surge to around 15 BCM in August. Subsequently, the discharge demonstrated a near-linear decline until December, highlighting the dynamic and predictable nature of the hydrological patterns within the region. If the monthly discharge from January to June is assumed to have an average of 0.5 BCM, the annual yield from the Blue Nile could be approximated as= 0.5 (BCM/month) * 6 (months) + 0.5 * 15 (BCM/month) * 6 (months) = 48 BCM/year which is close to the observed annual discharge of 48.5 BCM/year seen in Table (1).

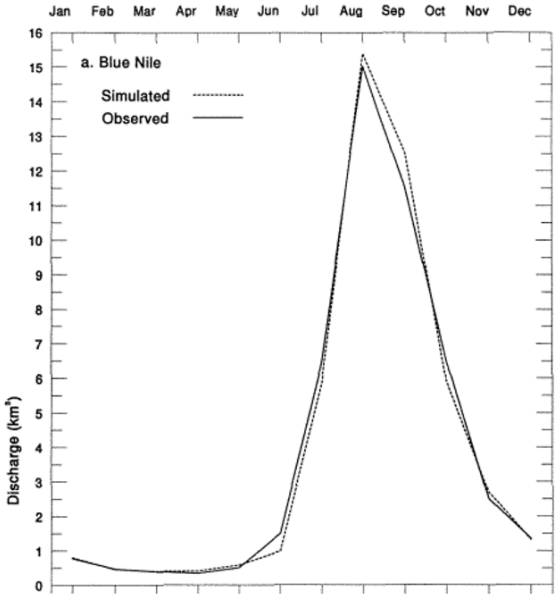

Fig. 5: Simulated (1951-1987) and observed (different periods) mean monthly runoff for calibration period: (a) the whole Upper Blue Nile (1951-1987), after Conway (1997)

Table 1: Validation results of time series simulation. Monthly correlation coefficients are calculated from standardized departures from the long-term monthly means, after Conway (1997)

	Mean annual discharge (km^3)		RMSE (km^3)		% RMSE		Max. error (km^3)		Correlation coefficient	
	Obs.	Sim.	Ann.	Mon.	Ann.	Mon.	Ann.	Mon.	Ann.	Mon.
76 years (1912–1987)	48.5	49.7	6.8	1.4	14.0	39.7	-19.8	-9.3	0.74	0.38
37 years (1951–1987)	47.4	46.2	5.8	1.3	12.2	34.5	-12.1	-9.3	0.79	0.4

Mohamed et al. (2005) present the result of a regional coupled climatic and hydrologic model of the Nile Basin. Interestingly the interaction between the climatic processes and the hydrological processes on the land surface has been fully coupled. The hydrological model is driven by the rainfall and the energy available for evaporation generated in the climate model and the runoff generated in the catchment is again routed over the wetlands of the Nile to supply moisture for atmospheric feedback. The Regional Atmospheric Climate MOdel (RACMO, Lenderink et al., 2003) is run over the Nile for the period 1995 to 2000. The results obtained are quite satisfactory given the extremely low runoff coefficients in the catchment, Mohamed et al. (2005). They presented the validation results over the sub-basins: Blue Nile, White Nile, Atbara River, the Sudd swamps and the Main Nile for the period 1995-2000. They found that the monthly moisture recycling ratio (i.e. locally generated/total precipitation) over the Nile varies between 8 and 14%, with an annual mean of 11%, which implies that 89% of the Nile water resources originates from outside the basin physical boundaries. The monthly precipitation efficiency varies between 12 and 53% and the annual mean is 28%. They report that inspection of the river discharge data shows also for comparison between model results and observations on a monthly time scale-that no correction for travel time was deemed necessary. They found that the mean annual runoff coefficient R (runoff)/P (precipitation) of observed P and R in 1995-2000 for the Main Nile, Atbara, White Nile and the Blue Nile are 0.05, 0.16, 0.02 and 0.19, respectively and the corresponding results derived from

DOI: 10.3844/ajessp.2025.49.78

their model are 0.14, 0.17, 0.09 and 0.29. Considering data uncertainty these results could be accepted.

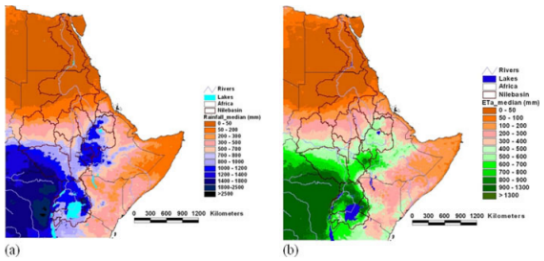

Fig. 6: Annual satellite-derived rainfall (median of 2001–2007) and (b) ETa estimate for the same time period, after Senay et al. (2009)

Senay et al. (2009) used satellite-derived rainfall and other key weather variables derived from the Global Data Assimilation System to estimate and map the distribution of rainfall, as seen in Figure (6a), the actual evapotranspiration (ETa) as seen in Figure (6b) and the runoff. Daily water balance components were modelled in a grid-cell environment at 0.1 degree (~10 km) spatial resolution; for 7 years from 2001 through 2007. Daily estimates of RFE, ETa and runoff were summed to an annual value for each of the 7 years from 2001-2007. The spatial distribution of the major water balance components were represented using the median values from the 7-year annual totals on a pixel-by-pixel basis. The median values were chosen from the average to reduce the influence of some extreme values from the relatively short time-series dataset. Annual maps of the key water balance components and derived variables such as runoff and ETa as a percent of rainfall were produced. Generally, the spatial patterns of rainfall and ETa indicate high values in the upstream watersheds (Uganda, southern Sudan and southwestern Ethiopia) and low values in the downstream watersheds. However, runoff as a percent of rainfall is much higher in the Ethiopian highlands around the Blue Nile sub-watershed. The analysis also showed the possible impact of land degradation in the Ethiopian highlands in reducing ETa magnitudes despite the availability of sufficient rainfall. Although the model estimates require field validation for the different subwatersheds, the runoff volume, Figure (7), estimate for the Blue Nile subwatershed is within 7.0% of a figure reported from an earlier study by Conway (1997); Senay et al. (2009). The model for the water yield of the Blue Nile resulted in 44.0 BCM (after being corrected to have the same area of 176,000 km³) compared to Conway (1997) who using this area obtained 47.4 BCM with a -7% difference. Senay et al. (2009) concluded that further research is required for a thorough validation of their results and their integration with ecohydrologic models for better management of water and land resources in the various Nile Basin ecosystems. Abera et al. (2017) report that the area of the Blue Nile River basin enclosed by a section at the Ethiopia–Sudan border is about 175,315 km³, covering about 17 % of the total area of Ethiopia. While Belete et al. (2018) considered the Blue Nile Basin to have a total catchment area of about 319,831 km^2 while Kamel et al. considered basin area of 314,000 km³ and the catchment area of the Blue Nile basin is about 325,000 Km³ according to Abdel-Aziz (2014). Indeed such a disparity of an important figure such as the Blue Nile catchment area highlights the difficulty in obtaining accurate and reliable data.

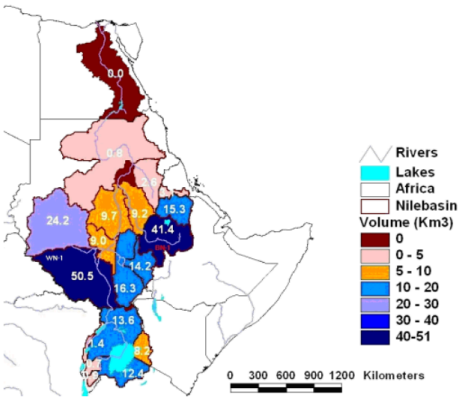

Fig. 7: Annual runoff volume estimate by subwatershed in km³ (median of 2001–2007), after Senay et al. (2009)

Abdel-Aziz (2014) forecasts hydrological process scenarios in Blue Nile basin using a Distributed Hydrological Model (DHM) and predicted scenarios of precipitation from two general circulation models, CCSM3 model and Miroc3.2-hires. Firstly, river discharge was simulated by the DHM using the observed rainfall from 1976-1979 and then, simulating future precipitations from 2011-2040, discharge scenarios were predicted. To simulate the current and long-term discharge dynamics for the river basin, the DHM geomorphology-based hydrological model (GBHM, Yang et al. (2002)) is used. This model's features were physically based on hydrological processes. That is, the water budget at each computational unit was simulated by a hill-slope module and the lateral inflow was routed downstream by a kinematic wave module. The discharge at each gauge point was obtained. A 4-km grid is chosen as computational units. Each computational unit is viewed as a rectangular inclined plane with a defined length and unit width. The inclination angle was given by the surface slope and the bedrock was assumed to be parallel to the surface. The hill-slope element introduced by Yang et al (2002) is used. The hill-slope module is applied in computational units having this feature. The module is divided into four parts: Storage of precipitation in the soil; precipitation storage in the canopy; water exchange between the saturated layer, unsaturated layer and the surface; and evapotranspiration from the canopy and the soil. Richard's equation is used

DOI: 10.3844/ajessp.2025.49.78

to calculate the water exchange between the saturated and unsaturated layers (Van Dam et al., 2000). Darcy's law is used to calculate the water flow in the saturated zone (Manning, 1997). To simulate transpiration, the Normalized Difference Vegetation Index (NDVI) from Advanced Very High Resolution Radiometer (AVHRR) is used to obtain the canopy cover ratio in each computational unit. The land use type and soil type from the USGS and FAO data determined each parameter of each hill-slope equation and each parameter is calibrated for each type of soil and land use. The simulated discharge flowing from each computational unit is accumulated into interval flows, which were identified according to the Pfafstetter Basin Numbering System. The accumulated discharge is routed from the upper to the lower basin according to the Pfafstetter numbering scheme by using the kinematic wave module. Thus, the discharge at each control point was obtained (Abdel-Aziz, 2014). Figure (8) shows discharge simulation at Khartoum Station using Rain gauge data where excellent agreement between the model results and the observed data is attained.

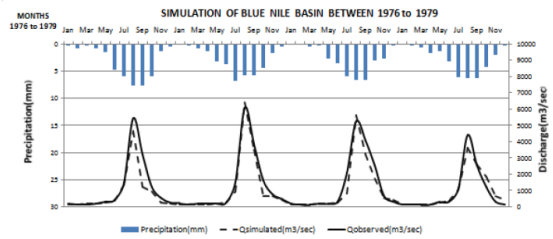

Fig. 8: Discharge simulation at Khartoum Station using Rain gauge data, after Abdel-Aziz (2014)

Wheeler et al. (2016) used "RiverWare" model to analyze strategies for filling the Grand Ethiopian Renaissance Dam and implications for downstream water resources. Their study considered a single hydrologic inflow node on each of the Blue and White Nile tributaries and included the GERD and High Aswan Dam (HAD), but contained no information on Sudanese reservoirs or any intervening flows. The RiverWare model of the Eastern Nile developed for this study was structured to contain all the major features in the basin that significantly affect water management and distribution, including: Lake Tana, with the Tana-Beles Hydropower Project and Tekeze Reservoir in Ethiopia; the Rosaries, Sennar, Jebel Aulia, Khashim El Girba and Merowe reservoirs in Sudan; and Lake Nasser/Lake Nubia, formed by the HAD, in Egypt. The recently raised Rosaries Dam, the newly developed Upper Atbara and Setit Dam complex and the GERD are included in simulations of future conditions. Monthly naturalized hydrologic input locations include 162 inflow nodes in South Sudan, Ethiopia, Sudan and Egypt. Demand locations reflect the major Sudanese diversion structures of the Gezira-Managil, New Halfa and Rahad schemes, as well as the minor diversions from the Jebel Aulia Reservoir and small aggregated demands between gauged locations. Consumptive or non-consumptive water uses within Egypt are not modelled beyond expected monthly releases from the HAD and necessary spills into the Toshka diversion works. Wheeler et al. (2016) generated 224 combinations of policies and initial conditions, each being subject to 103 hydrologic traces, thus requiring around 23,000 simulations (Wheeler et al. 2016).

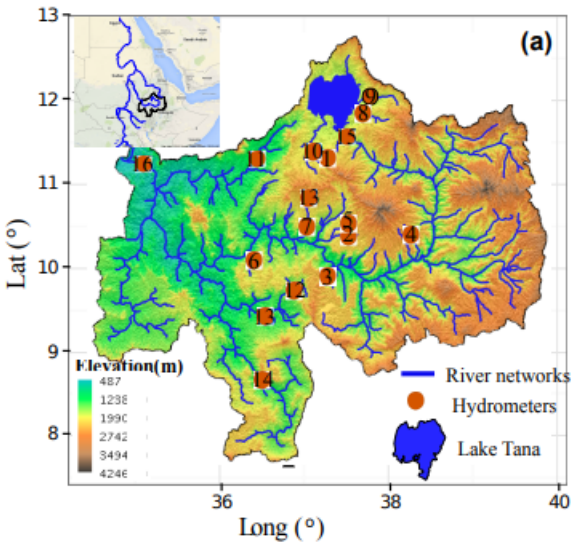

Fig. 9: The Upper Blue Nile basin digital elevation map, along with the gauge stations present in the basin. Numbers inside the circles designate the river gauging stations, after Abera et al. (2017)

Abera et al. (2017) developed a methodology that can improve the state of the art by using available, but sparse, hydro-meteorological data and satellite products to obtain the estimates of all the components of the hydrological cycle (precipitation, evapotranspiration, discharge and storage) of the Upper Blue Nile Basin, Figure (9). To obtain the water-budget closure, they use the JGrass-NewAge system and various remote sensing products. The satellite product SM2R-CCI is used for obtaining the rainfall inputs, SAF EUMETSAT for cloud cover fraction for proper net radiation estimation, GLEAM for comparison with NewAge-estimated evapotranspiration and GRACE gravimetry data for comparison of the total water storage amounts available in the whole basin. Results are obtained at daily time steps for the period 1994–2009 (16 years) and they can be used as a reference for any water resource development activities in the region. The overall water-budget analysis shows that precipitation of the Upper Blue Nile basin is 1360±230 mm per year. Evapotranspiration accounts for 56 % of the annual

DOI: 10.3844/ajessp.2025.49.78

water budget and runoff is 33 %, storage varies from −10 to +17% of the water budget, Abera et al. (2017). Their model results of the long-term basin-average water-budget components show 1360±230 mm of precipitation (P), followed by 740±87 mm of ET, 454±160 mm of Q and −4±63 mm of ds / dt. While the spatial variability of the water budget is high, the annual variability is rather limited. Higher annual variability is observed for precipitation, followed by Q. 2001 and 2006 are wet years, characterized by high precipitation and Q. Conversely, 2002 and 2009 are dry years with 1167 mm and 1215 mm per year of precipitation. The study covered 16 years from 1994 to 2009 at a finer spatial and temporal resolution.

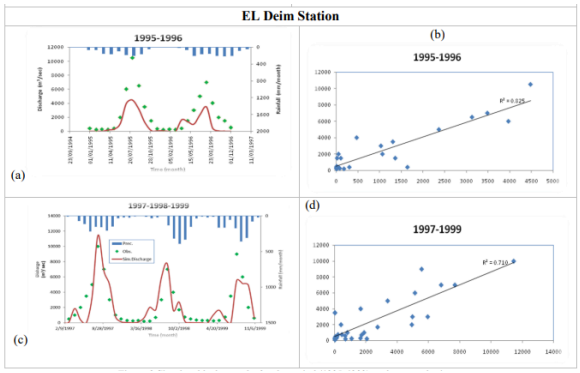

Fig. 10: Simulated hydrographs for the period (1995-1999) at outlet station of the Blue Nile Basin (El Diem station), after Abd-El Moneim et al. (2017)

Abd-El Moneim et al. (2017) used the Hydrological River Basin Environmental Assessment Model (HydroBEAM) to simulate the surface discharge in the Blue Nile Basin during the period (1995-1999) using a long-term global atmospheric reanalysis product, namely Japanese 25-year reanalysis (JRA-25). These data include precipitation, temperature, pressure, wind speed, specific humidity, downward short-wave radiation, upward short-wave radiation, downward long-wave radiation and upward long-wave radiation. Hydro-BEAM was originally developed by Kojiri et al (1998) as a tool to assist in simulating long-term fluctuations in water quality and quantity in rivers through an understanding of the hydrological processes that occur within a watershed. Hydro-BEAM is a physical-based distributed hydrological model that is adapted to simulate surface runoff in Blue Nile Basin. It consists of: (1) the watershed modeling using Geographical Information System (GIS) technique, (2) Surface runoff and stream routing modeling based on the kinematic wave approximation, (3) Canopy interception losses and (4) Groundwater modeling based on the linear storage model. The watershed is divided into meshed cells with multi layers and each mesh contains information such as surface runoff, land use, slope direction and the absence/ presence of a channel. The spatial resolution used to model the Blue Nile Basin is (5×5 km). The simulated discharge was examined and calibrated at Khartoum, Sennar dam and El Deim gauging stations. Good agreement obtained between the observed and the simulated discharge as seen in Figure (10), for the outlet station of the Blue Nile Basin: El Diem station.

Belete et al. (2018) explored the applicability of a simple water budget model, the Integrated Valuation of Environmental Services and Tradeoffs (InVEST) annual water yield model, to the Nile Basin. InVEST is a collection of open-access and freely available software models used to map and value ecosystem services. The InVEST annual water yield model was selected for their study due to its low input data requirements, ease of use and simple model calibration.

The InVEST annual water yield model assumes that all water in excess of evaporative loss is runoff or water yield. It requires nine tabular and biophysical parameters, such as precipitation, evapotranspiration and land use/cover data, which can be obtained from globally available datasets. The study used InVEST version 3.3.3 to simulate the annual mean water production of the Nile River Basin, which was divided into 10 sub-watersheds as seen in Figure (11). InVEST calculates water production at a pixel level to capture the heterogeneity of the landscape but reports results at the watershed or sub-watershed level, as in Figure (11) and Table (3).

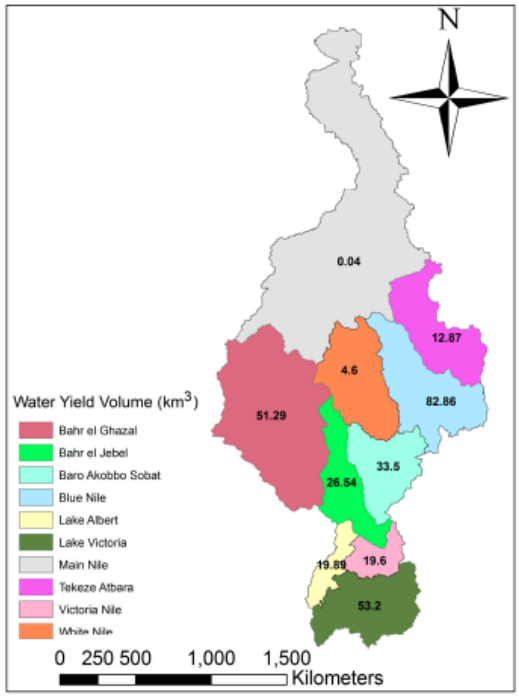

Fig. 11: Annual average water yield volume estimated by sub-watershed in km3 (Billion m3), after Belete et al. (2018)

Table 3: Meso-scale hydrological model (mHM) global datasets used for the model (Lorenz et al., 2019), after Hassan et al. (2023)

Product	Dataset Name	Developing Institute	Websites
DEM	Global Multi-resolution Terrain Elevation Data (GMTED2010)	US Geological Survey (USGS) and National Geospatial-Intelligence Agency (NGA)	https://topotools.cr.usgs.gov/gmted_viewer/gmted2010_global_grids.php
Soil	SoilGrids	Wageningen University	ftp://ftp.soilgrids.org/data/recent/
Geology	Global Lithological Map (GLiM)	Institute for Biogeochemistry and Marine Chemistry, KlimaCampus, Universität Hamburg	https://doi.pangaea.de/10.1594/PANGAEA.788537
Land cover	Global Land Cover (GlobCover)	European Space Agency (ESA), Université Catholique de Louvain	http://due.esrin.esa.int/files/Globcover2009_V2.3_Global_.zip
Leaf area index (LAI)	Global Inventory Modelling and Mapping Studies (GIMMS)	Global Land Cover Facility, University of Maryland	http://iridl.ldeo.columbia.edu/SOURCES/.UMD/.GLCF/.GIMMS/.NDVIg/.global/

The key findings of the study are:

1. The annual average water yield for the Nile River Basin is estimated to be 304.51 km³, with substantial spatial variation ranging from 0.04 km³ in the Main Nile sub-watershed to 82.86 km³ in the Blue Nile sub-watershed
2. The highest water yields are generated from the Blue Nile, Lake Victoria and Bahr el Ghazal sub-watersheds, while the northern sub-watersheds contribute negligibly
3. The study confirms the ability of the InVEST water yield model to estimate annual water yield production in the data-scarce Nile Basin without the need for flow meters
4. The model helps to prioritize which parts of the basin should be managed to maximize the water production ecosystem service

However, the study acknowledges several limitations of the InVEST model:

1. It does not consider storage effects within the basin, such as in lakes, wetlands and swamps
2. The calculated water yield may be higher due to the neglect of groundwater flows or seepage losses
3. The sub-watershed areas used in the study differ from previous studies, leading to differences in water yield estimates
4. The model does not indicate the fraction of water yield that is stored within each sub-watershed versus the fraction that is transported to downstream units
5. The flow paths and hydrological connectivity between the sub-watersheds are not shown

The study justifies the use of the simple InVEST model in the Nile Basin, where complex hydrological models are difficult to apply due to the lack of observed data for input, calibration and validation. The authors argue that the results of simple models are often more accurate than complex models in data-scarce regions, as concluded by previous studies (Bashar et al. (2005) and Awulachew et al. 2008).

Overall, this study introduces the InVEST water yield model as a user-friendly tool that can be used by non-technical stakeholders to evaluate the impact of land use changes on water production in the Nile Basin, where data scarcity is a major challenge for applying more complex hydrological models.

Kamel et al. (2019a) reported that the developed water allocation model called Eastern Nile Model (ENM) using RiverWare software, has proved its worth application on the ENM. They realized that the effective use of Riverware tools in ENM requires the updating of hydrological conditions, but the hydrological data in ENM ceased in 2002, casting doubt on the possibility of using it for recent periods. In their study, the hydrological conditions in the model were updated from 2003-2014 with a simulated flow data, which were taken from the output of rainfall-runoff distributed model (Nile Forecast System (NFS), 2012). The shortage of the observations in the Nile catchment leads to use a simulated data in order to update the ENM. The simulated data were taken from the NFS output. The main control points on the Nile stream are located in the NFS schematic that run the hydrological models and introduce simulation flows at each feeding control point. The ENM schematic contains 162 control points; each control point represents the flow from small tributary catchment. The control point flow is the main input for the model and it can be fed by observed, simulated or forecasted information. The available flow data in the model database is made of monthly time series from 1900 till the end of 2002. In order to update the ENM, the control flow points in the model will be updated from 2003 to 2014 by simulated flow data produced from Nile Forecast System (NFS). The NFS is a hydro-meteorological distributed model, which simulate the Nile flow till the Dongala station (the end point before flow entering Lake Nasser) as seen in Figure (12). The main inputs of NFS are: the rainfall which estimated from the satellite images and merged with observed rain gauge data and the observed mean monthly

DOI: 10.3844/ajessp.2025.49.78

evapotranspiration. The main hydrological models in NFS are; water balance, hill-slope and river routing models. The ENM evaluation was performed by comparing the simulated with the observed outflows at the locations of Diem, Khartoum and Dongola stations using statistical criteria where all metrics were considered very good or good (Kamel et al. (2019a)) as seen in Figure (13). The updated ENM was used by Kamel et al. (2019b) to simulate the filling and operation of GERD reservoir in RiverWare software. The ENM simulation was accomplished for three scenarios (initial HAD level 165, 170, 175 m). The number of the hydrological flow ensembles for each scenario was 115; the length of the ensemble was for the period (2017-2060).

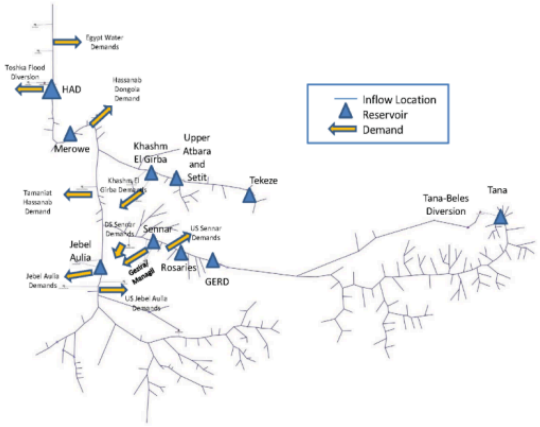

Fig. 12: Eastern Nile schematic as developed in the RiverWare software, after Kamel et al. (2019a)

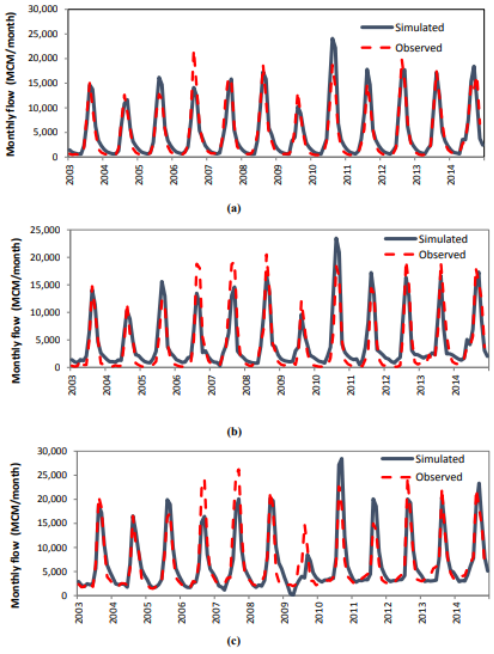

Fig. 13: The comparison of the RiverWare simulation flow and observed flow data at (a) Diem station; (b) Khartoum station; (c) Dongola station, after Kamel et al. (2019a)

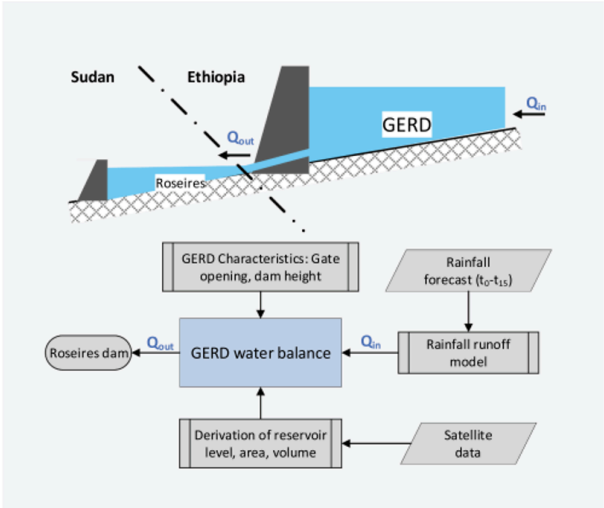

Fig. 14: Analytical framework for computing river inflow into the Rosaries reservoir, after Hassan et al. (2023)

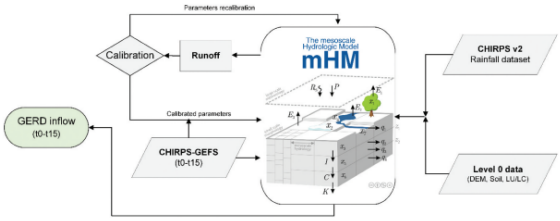

Fig. 15: Structure of the meso-scale hydrological model (mHM), after Hassan et al. (2023)

Hassan et al. (2023) used a water balance model (Meso-scale hydrological mode: mHM) to predict the Grand Ethiopian Renaissance Dam (GERD) releases and the dates of overtopping during subsequent fillings events. The unexpected drop of the Blue Nile water in July 2020, attributed to the sudden closure of GERD during the first filling in 2020, significantly interrupted the water supply for Khartoum, Sudan. This incident pursued using satellites and hydrological models to estimate inflows into Rosaries dam as seen in Figure (14). Reservoir levels were extracted from Sentinel1, -2 and Jason-3. The study demonstrates the effectiveness of satellite data and models for transboundary reservoir management. The Meso-scale hydrological model (mHM) is a fully distributed, grid-based to compute inflow into the GERD reservoir (Samaniego et al., 2011). The mHM model was selected because of previous experience of the team in both the Blue Nile and Tekezze–Atbara basins. It is an open-source conceptual model simulating rainfall-runoff process (Figure 15). The model was set up using the global database as seen in Table (4) with a spatial resolution of 0.002°. Initial model parameters were obtained from spatially disaggregated ERA5 climate re-analysis data (Lorenz et al., 2019). Using historical precipitation datasets of CHIRPS (the Climate Hazards Centre InfraRed Precipitation with Stations data, Ethiopia) and measured

DOI: 10.3844/ajessp.2025.49.78

discharges at El-Deim station, the mHM model for the upper Blue Nile was calibrated and validated for the periods 2002–06 and 2007–11, respectively. The results show very good performance for both calibration and validation periods, as given in Figure (16). This model is under the category of Blue Nile Basin models.

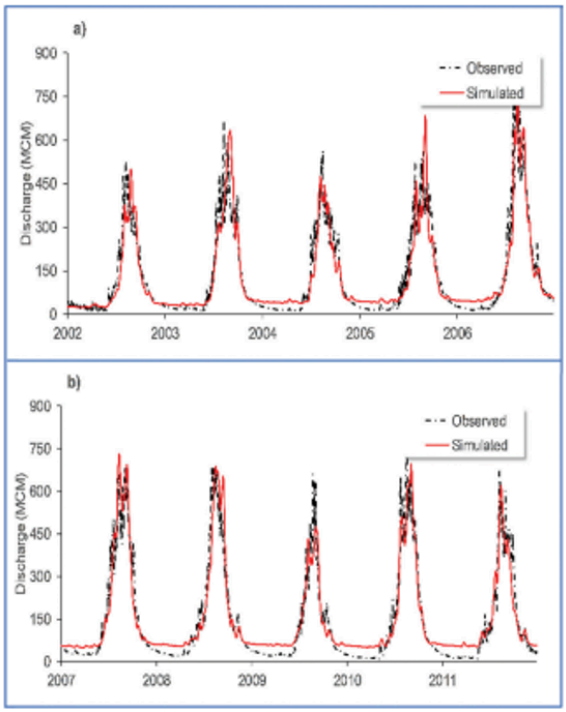

Fig. 16: Observed and simulated daily discharges at El–Deim station computed by the meso-scale hydrological model (mHM) derived by CHIRPS dataset: (a) calibration and (b) validation, after Hassan et al. (2023)

The foregoing review shows that physically based hydrologic models requires a lot of detailed data where either some data are not hard to measure and some are not available. This leaves water budget models to provide important flow information with the least amount of data. In the following is a description of proposed water budget model that requires minimum data structure and provide the basic required flow balances and connectivity between the various flow hydrological units in the Nile River basin.

River Basin Flow Model (RBFM)

Model Overview

The RBFM model simulates the water balance of a river basin by dividing it into interconnected units. Each unit represents a distinct hydrological entity, such as a lake, reservoir, or river reach. The model operates on a yearly basis due to data availability and the usual complexity of river basin systems such as the Nile Basin system. The model development described here is associated with its application to the Nile River Basin to make the presentation more practical.

Model Components

Units

To cover the Nile Basin (based on the schematization by Abul-Atta in 1978) from Lake Victoria to Lake Nasser in Egypt, the Nile Basin model uses 35 units, representing key hydrological features as was shown in Figure (3).

For the current Nile basin conditions that include several dams which were not present in the previous Nile basin schematization, such as the Grand Ethiopian Renaissance Dam (GERD), Tekeze Dam, Setit Dam, Khashm El Girba Dam, Merowe Dam and Toshka Inlet, the model uses 48 units as shown in Figure (17).

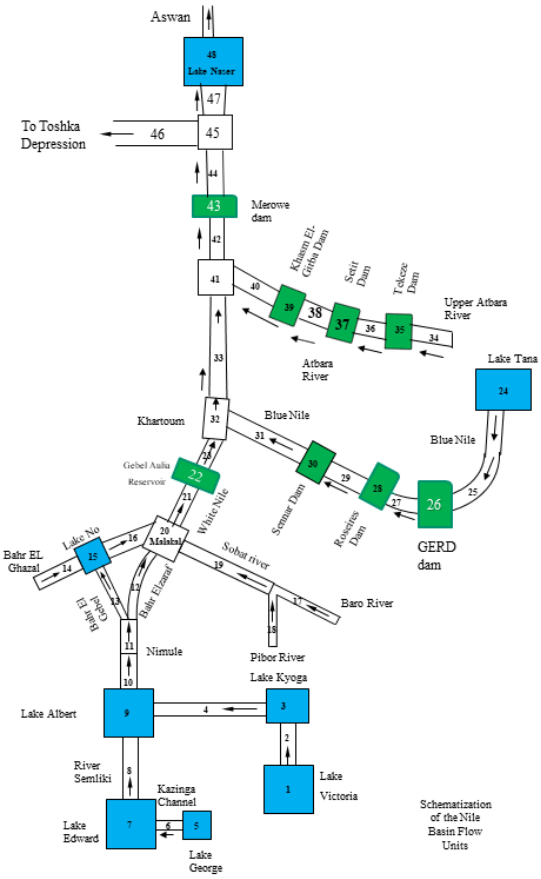

Fig. 17: Nile Basin model with 48 units (for current conditions including dams) [Nile Basin model with 48 units]

Examples of the units in the model include Lake Victoria (Unit 1), Lake Kyoga (Unit 3) and the Nile-Victoria-Kyoga river channel (Unit 2).

Water Sources

Distributed Sources:

- Direct rainfall on the unit itself (m/year) considered as distributed water source.
- Rainfall from connected catchments, expressed as rainfall depth (m/year).

Point Sources:

- Inflow from upstream river reaches (Million m^3/year).
- Tributary flows from side channels (Million m^3/year).
- Drainage channels discharging into the unit (Million m^3/year).

Water Sinks

Distributed Sinks:

- Evaporation from the unit's surface (m/year).
- Seepage through the unit's floor (m/year).

Point Sinks:

- Water abstractions for irrigation canals or drinking water plants (Million m^3/year).
- Water storage in lakes or dam reservoirs (Million m^3/year).

Data Requirements

For each unit:

- Area (km^2).
- Depth (m).
- Width (m).
- Length (m).
- Slope (m/m).
- Elevation (m).
- Rain rate (m/year).
- Evaporation rate (m/year).
- Seepage rate (m/year).
- Number of connected catchments.
- Number of point source inflows and their inflow rates (Million m^3/year).
- Number of point source outflows and their outflow rates (Million m^3/year).

For each connected catchment:

- Area (km^2).
- Rainfall rate (m/year).
- Losses (evaporation, seepage, etc.) (m/year).
- Runoff coefficient (0 to 1.0) which reflects land use and cover.

For each connected upstream unit:

- Flow rate (m^3/year).
- Delivery ratio (0 to 1.0).
- Reach loss coefficient (0 to 1.0)

Model Calculations

Inflow from connected catchments:

- Catchment inflow = Catchment area * (Rainfall rate - Losses) * Runoff coefficient
- Losses are due to evapotranspiration, seepage to soil & canopy interception …etc.
- Runoff coefficient = C

Inflow from connected upstream units:

- Upstream inflow = Upstream unit outflow * Delivery ratio

Total inflow to the unit:

- Total inflow = Catchment inflow + Upstream inflow + Sum of point source inflows

Unit outflow:

- Unit outflow = (1 - Unit loss) * (Unit area * (Rain rate - Evaporation rate - Seepage rate) + Total inflow - Sum of point source outflows - Water storage)

Nile Basin water yield:

- The model calculates the outflow from each unit sequentially, culminating in the Nile Basin water yield at Lake Nasser.

Model Applications and Limitations

The model quantifies the effects of climatic conditions (via rainfall and evaporation) and land use (via runoff coefficient) on the Nile Basin water balance.

Due to data limitations, the model currently operates on a yearly basis.

The modeling structure allows the model to simulate monthly, 10 days. For daily time steps the travel time of the flows between the units is an additional required data.

Results and Discussion

The Nile Basin, schematized in Figure (3) using 35 units, extends from Lake Victoria in the south to Lake Nasser in Egypt in the north. This representation, based on Abul-Atta's (1978) description, reflects conditions prevailing in the 1970s. Consequently, it does not include dams constructed after that period, such as GERD, Tekeze, Setit, Khasm El Girba and Merowe. However, it incorporates the Gebel-Aulia, Rosaries and Sennar Dams, which were operational at the time. The rainfall conditions correspond to average flood levels, resulting in an estimated water yield of approximately 84 BCM at Lake Nasser in Aswan, Egypt.

Multiple studies, including those by Abul-Atta (1978), Sutcliffe and Parks (1999), Ribbe and Ahmed (2006), Sayed (2008), AbuZeid (2019) and Mahmoud et al. (2022), consistently report the total Nile Basin water resources as around 84 BCM/year of runoff measured at the Aswan High Dam.

Table (6) presents the flow calculations from the RBFM model for various units. Notably, the outflow at Lake Victoria is approximately 24 BCM, which remains consistent throughout the Equatorial lakes and Sudd regions, reaching the White Nile with the same volume. The Blue Nile yield at El-Diem station amounts to 50

BCM, contributing to a final Nile Basin yield of 84.112 BCM at Lake Nasser. The ratio of the Blue Nile Basin yield to the main Nile yield at Aswan (50/84.1 = 0.595) aligns with Abu-Zeid and Biswas's value of 0.6. The Rahad and Dinder tributaries are estimated to contribute an additional 4 BCM/year, bringing the total Blue Nile basin yield at Khartoum to 54 BCM/year.

For the Baro River reach (unit 17) before its confluence with the Pibor River, a flow of 13 BCM/year is used with a reach loss of 0.29, resulting in a net flow of 9.23 BCM/year. The Pibor River (unit 18) is assumed to have a flow of 2.8 BCM/year. Downstream of the confluence of the Baro and Pibor Rivers (unit 19), two tributary flows of 1.1 and 0.4 BCM/year are considered. The net flow for the Sobat River then becomes 9.23 + 2.8 + 0.4 + 1.1 = 13.53 BCM/year.

Lake Tana (unit 24) is characterized by a rainfall rate of 1.267 m/year and an area of 3000.0 km², yielding 3.8 BCM/year. Due to the lack of available data for tributaries in the reach between Lake Tana and GERD, eight point source tributary inflows, each with 5775 Million m3/year, are assumed, totaling 46.200 BCM/year. Adding this to the 3.8 BCM/year from Lake Tana, the total flow at the GERD location or El-Diem station becomes 50 BCM/year. The Upper Atbara River at the Tekeze dam (unit 34) has an inflow of 12 BCM/year, which flows through the entire Atbara River (unit 32) until it meets the main Nile at Atbara city.

Sutcliffe and Parks (1999) report mean river natural flows for the period ~1910 to 1995, as shown in Table (4): 16.1 BCM for the Sudd wetland at Malakal, 26.0 BCM for the White Nile at Khartoum, 48.3 BCM for the Blue Nile at Khartoum, 11.1 BCM at Atbara and 84.1 BCM for the main Nile River at Aswan. These values closely align with the corresponding RBFM model results of mean annual flows: 15.6 BCM at Malakal (7.56 BCM from Bahr El Zaraf (unit 12) plus 8.06 BCM from Lake No (unit 16)), 24.1 BCM for the White Nile at Khartoum, 50 BCM for the Blue Nile at El Diem and 13.1 BCM for the Atbara River at Atbara. Wheeler et al. (2016) report the average annual flow at the GERD dam location (representing the water yield from the Blue Nile) as 49.4 BCM, while the RBFM model yields 50.001 BCM.

Mahmoud et al. (2022) indicate that the 1993–1994 hydrologic year corresponds to a normal natural flow of 84 BCM at the HAD. They further report annual flows at specific locations: (a) 75.34 BCM measured at the Dongola gauge; (b) 23.16 BCM released from Jabal Al Awlia; (c) 7.21 BCM measured at the Atbara River; and (d) 53.92 BCM (~ 54 BCM) measured at the El Diem gauge. They also report that the 1998–1999 hydrologic year represents a "high flood," with annual flows at specific locations: (a) 107.04 BCM measured at the Dongola gauge; (b) 28.23 BCM released from Jabal Al Awlia; (c) 17.76 BCM measured at the Atbara River; and (d) 68.40 BCM measured at the El Diem gauge.

Shahin (1998) reports that the peak discharge of the 1946 Nile flood at the Aswan gauge station was approximately 32,000 m³/s, over 10 times the average annual Nile River discharge of around 2,800 m³/s. This flood caused widespread devastation and damage along the river valley in Egypt, highlighting the immense power and variability of the Nile's seasonal flooding regime. This event was a key factor behind Egypt's decision to construct the High Aswan dam to mitigate the risks of such extreme floods. Understanding and mitigating the impacts of these floods remains a crucial challenge for the countries and communities along the Nile River. According to the National Oceanic and Atmospheric Administration (NOAA), the highest annual flood for the Nile River was recorded in 1964, with a discharge volume of approximately 62,000 m³/s. This extraordinary flooding was caused by heavy rainfall in Ethiopia and Kenya. Unfortunately, complete data sets for rainfall, evaporation and seepage losses, among other factors, are not readily available to comprehensively test the developed model.

Now the study utilizes the River Basin Flow Model (RBFM) to simulate flow conditions in the Nile Basin, incorporating existing dams and exploring various hydrological scenarios. The model was applied to a schematization of the Nile Basin, representing the current state of the basin, including major dams like GERD, Tekeze, Setit, Khasm El Girba and Merowe in addition to Toshka intake as seen in Figure (17). The RBFM was run under different hydrological conditions, with varying input data for the Blue Nile and Atbara River. Lack of sufficient and accurate data for dam operations (especially GERD) and their associated hydrology prohibited their inclusion in detailed analyses and this is left for future studies.

The model uses a connected catchment area of 176,000 km² (cases S2 to S7) for the reach between Lake Tana and GERD (Unit 25), specified rainfall rates, losses due to evaporation and a runoff coefficient. For the Upper Atbara and Tekeze reach (Unit 34), the model uses a catchment area of 248,219.0 km², rainfall of 0.477 m/year, losses (evaporation) of 0.424 m/year and a runoff coefficient of 1.0, resulting in a flow discharge of 13.155 BCM/y routed through units 35 to 40 until it reaches the main Nile River at Atbara city.

The study explores eight different cases (S1-S8, shown in Table 6) based on various data sources. Case S1 uses Abu-Atta 1978 data, similar to the results in Table (5). Case S2 is similar to S1 but with a Blue Nile catchment area of 176,000 km² (Conway 1997), while the precipitation (p) = 1.041 m/year, actual evapotranspiration (AET) = 0.781 m/year and C = 1.0 are according to Belete et al. (2018) as shown in Table (2). Case S3 uses data representing maximum conditions

according to Abera et al. (2017) with p = 1.59 m/year, AET = 0.827 m/year and C = 0.33. Case S4 employs average values reported by Abera et al. (2017) with p = 1.36 m/year, AET = 0.74 m/year and C = 0.33. Case S5 uses the lower limits of the data in Abera et al. (2017) with p = 1.13 m/year, AET = 0.653 m/year and C = 0.33. Case S6 is the same as S3 but with p = 2.0 m, representing a climate change scenario assuming heavy rain. Case S7 has p = 0.9 m/y, AET= 0.653 m/y and C = 0.33, representing a climate change scenario assuming small rain. Case S8 is similar to case S2 but with a Blue Nile catchment area of 319,813 km² (Belete et al., 2018). The runoff coefficient was taken as 1.0 in the S2 and S8 cases as no reported data was found.

Table 5: Flows at the Nile Basin Units at Conditions according to Abul-Atta (1978); BCM = Billion cubic meter

Unit Number as in Figure (3)	Unit Location	Unit Annual Flow in BCM/year
1	Lake_Victoria	24.0169
2	Nile_Victoria_Kyoga	24.0169
3	Lake_Kyoga	22.9359
4	Nile_Kyoga_Albert	22.9359
5	Lake_George	0.00E+00
6	Kazinga_Channel	0.00E+00
7	Lake_Edward	2.50008
8	River_Semliki	3.99608
9	Lake_Albert	26.89722
10	Albert_Nile	26.22479
11	Bahr_ElGebel_Nimule	30.24917
12	Bahr_El_Zaraf	7.562293
13	Bahr_ElGebel_Mongalla	7.562293
14	Bahr_El_Arab	5.00E-01
15	Lake_No	8.062293
16	Sudd_Lake_No_Malakal	8.062293
17	River_Baro	9.23
18	River_Pibor	2.8
19	River_Sobat	13.53
20	Malakal	29.15459
21	White_Nile	24.11084
22	Gabal_Auliaa_Dam	24.11084
23	White Nile_Auliaa_Khartoum	24.11084
24	Lake_Tana	3.801
25	Blue_Nile_Tana_Rosaries	50.001
26	Rosaries_Dam	50.001
27	Nile_Rosaries_Sennar	50.001
28	Sennar_Dam	50.001
29	Blue_Nile_Sennar_Khartoum	54.001
30	Nile_Khartoum	78.11185
31	Nile_Khartoum_Atbara	78.11185
32	Atbara_River	12
33	Nile_Atbara_Aswan	90.11185
34	Lake_Nasser_Inlet	84.11185

The results show varying Nile yields at Aswan, ranging from 53.4 BCM/year to 122 BCM/year. Cases 1 and 2 yield nearly identical results although the input data for the Blue Nile basin and Atbara are different which supports the validity of both of them. Case S3, using maximum conditions, predicts a Blue Nile yield of 48.116 BCM/y and a Main Nile yield at Aswan of 83.3825 BCM/y, closely resembling the mean river natural flows reported by Sutcliffe and Parks (1999). Case S4, using average conditions, produces a below-average yield, with a Blue Nile yield of 39.8 BCM/y and a Main Nile yield at Aswan of 75.08 BCM/y. Case S5 for the lower conditions yields BNB yield of 31.5 BCM/y and Nile yield at Aswan of 66.77 BCM/y. Abera et al. (2017) using the JGrass-NewAge model system and satellite data obtained runoff yield from the Blue Nile Basin of 0.614, 0.454 and 0.294 m/y for the maximum, average and minimum conditions. Using BNB area of 176,000 km³, these values correspond to yield of 108.1, 79.9 and 51.7 BCM/y versus corresponding values of the RBFM of 48.1, 39.8 and 31.5 BCM/y. The above values by Abera et al. (2017) seem to be high as according to AbuZeid (2019) the Blue Nile flows during the period from year 1911-2015 (105 years of records) shows a range from 20.69 BCM/y in year 1913 to 69.85 BCM/y in year 1929.

DOI: 10.3844/ajessp.2025.49.78

Table 6: Flows at the Nile Basin Units for current conditions that include 48 units

Unit Number Figure (17)	Unit Name or Location	S1 flows in BCM/y	S2 flows in BCM/y	S3 flows in BCM/y	S4 flows in BCM/y	S5 flows in BCM/y	S6 flows in BCM/y	S7 flows in BCM/y	S8 flows in BCM/y
1	Lake_Victoria	24.0169	24.0169	24.0169	24.0169	24.017	24.0169	24.017	24.0169
2	Nile_Victoria_Kyoga	24.0169	24.0169	24.0169	24.0169	24.017	24.0169	24.017	24.0169
3	Lake_Kyoga	22.9359	22.9359	22.9359	22.9359	22.936	22.9359	22.936	22.9359
4	Nile_Kyoga_Albert	22.9359	22.9359	22.9359	22.9359	22.936	22.9359	22.936	22.9359
5	Lake_George	0	0	0	0	0.000	0	0.000	0
6	Kazinga_Channel	0	0	0	0	0.000	0	0.000	0
7	Lake_Edward	2.50008	2.50008	2.50008	2.50008	2.500	2.50008	2.500	2.50008
8	River_Semliki	3.99608	3.99608	3.99608	3.99608	3.996	3.99608	3.996	3.99608
9	Lake_Albert	26.89722	26.89722	26.89722	26.89722	26.897	26.89722	26.897	26.89722
10	Albert_Nile	26.22479	26.22479	26.22479	26.22479	26.225	26.22479	26.225	26.22479
11	Bahr_ElGebel_Nimule	30.24917	30.24917	30.24917	30.24917	30.249	30.24917	30.249	30.24917
12	Bahr_El_Zaraf	7.56229	7.56229	7.56229	7.56229	7.562	7.56229	7.562	7.56229
13	Bahr_ElGebel_Mongalla	7.56229	7.56229	7.56229	7.56229	7.562	7.56229	7.562	7.56229
14	Bahr_El_Arab	0.5	0.5	0.5	0.5	0.500	0.5	0.500	0.5
15	Lake_No	8.06229	8.06229	8.06229	8.06229	8.062	8.06229	8.062	8.06229
16	Sudd_Lake_No_Malakal	8.06229	8.06229	8.06229	8.06229	8.062	8.06229	8.062	8.06229
17	River_Baro	9.23	9.23	9.23	9.23	9.230	9.23	9.230	9.23
18	River_Pibor	2.8	2.8	2.8	2.8	2.800	2.8	2.800	2.8
19	River_Sobat	13.53	13.53	13.53	13.53	13.530	13.53	13.530	13.53
20	Malakal	29.15459	29.15459	29.15459	29.15459	29.155	29.15459	29.155	29.15459
21	White_Nile	24.11084	24.11084	24.11084	24.11084	24.111	24.11084	24.111	24.11084
22	Gabal_Auliaa_Dam	24.11084	24.11084	24.11084	24.11084	24.111	24.11084	24.111	24.11084
23	Nile_Auliaa_Khartoum	24.11084	24.11084	24.11084	24.11084	24.111	24.11084	24.111	24.11084
24	Lake_Tana	3.801	3.801	3.801	3.801	3.801	3.801	3.801	3.801
25	Reach between Lake Tana and GERD	50.001	49.561	48.11604	39.8106	31.505	71.92884	18.147	86.95705
26	GERD	50.001	49.561	48.11604	39.8106	31.505	71.92884	18.147	86.95705
27	Reach between GERD and Rosaries Dam	50.001	49.561	48.11604	39.8106	31.505	71.92884	18.147	86.95705
28	Rosaries Dam	50.001	49.561	48.11604	39.8106	31.505	71.92884	18.147	86.95705
29	Reach between Rosaries and Sennar Dams	50.001	49.561	48.11604	39.8106	31.505	71.92884	18.147	86.95705
30	Sennar Dam	50.001	49.561	48.11604	39.8106	31.505	71.92884	18.147	86.95705
31	Between Sennar Dam and Khartoum	54.001	53.561	52.11604	43.8106	35.505	75.92884	22.147	90.95705
32	Khartoum	78.11185	77.67184	76.22689	67.92145	59.616	100.0397	46.258	115.0679
33	Reach between Khartoum and Atbara	78.11185	77.67184	76.22689	67.92145	59.616	100.0397	46.258	115.0679
34	Upper Atbara	12	13.15561	13.15561	13.15561	13.156	13.15561	13.156	13.15561
35	Tekeze Dam	12	13.15561	13.15561	13.15561	13.156	13.15561	13.156	13.15561
36	Between Tekeze and Setit Dams	12	13.15561	13.15561	13.15561	13.156	13.15561	13.156	13.15561
37	Setit Dam	12	13.15561	13.15561	13.15561	13.156	13.15561	13.156	13.15561
38	Between Setit and Khashm El Girba Dams	12	13.15561	13.15561	13.15561	13.156	13.15561	13.156	13.15561
39	Khashm EL Girba Dam	12	13.15561	13.15561	13.15561	13.156	13.15561	13.156	13.15561
40	Between Khashm El Girba Dam and Atbara	12	13.15561	13.15561	13.15561	13.156	13.15561	13.156	13.15561
41	Atbara Confluence with Main Nile	90.11185	90.82745	89.3825	81.07706	72.772	113.1953	59.413	128.2235
42	Between Atbara Confluence and Merowe Dam	90.11185	90.82745	89.3825	81.07706	72.772	113.1953	59.413	128.2235
43	Merowe Dam	90.11185	90.82745	89.3825	81.07706	72.772	113.1953	59.413	128.2235
44	Between Merowe Dam and Toshka	84.11185	84.82745	83.3825	75.07706	66.772	107.1953	53.413	122.2235
45	Toshka Station	84.11185	84.82745	83.3825	75.07706	66.772	107.1953	53.413	122.2235
46	Inlet to Toshka Depression	0	0	0	0	0.000	0	0.000	0
47	Toshka to Aswan Reach	84.11185	84.82745	83.3825	75.07706	66.772	107.1953	53.413	122.2235
48	Lake Nasser	84.11185	84.82745	83.3825	75.07706	66.772	107.1953	53.413	122.2235

S1 Data Abu-Atta 1978; S2 same as S1 but with Bule Nile catchment of area of 176,000 km 2 , p = 1.041 m/y, AET= 0.781 m/y, and C =1.0 (according to Conway 1997); S3 p = 1.59 m/y, AET = 0.827 m/y, C = 0.33 maximum conditions according to Abera et al. (2017), S4 p = 1.36 m/y, AET = 0.74 m/y, C = 0.33 average conditions according to Abera et al. (2017); S5 p = 1.13 m/y, AET = 0.653 m/y, C = 0.33 minimum conditions according to Abera et al. (2017); S6 same as S3 but with p =2.0 m; S7 p = 0.9 m/y, AET= 0.653 m/y, C = 0.33; S8 as S2 but with Bule Nile catchment of area of 319,813 km 2 according to Belete et al. (2018)

DOI: 10.3844/ajessp.2025.49.78

Table 7: Effects of changes in land cover area on Flows at the While Nile Basin (Units 1 to 23)

Unit Number Figure (17)	Unit Name or Location	S9 Base case flows in BCM/y	S10 flows in BCM/y	S11 flows in BCM/y	S12 flows in BCM/y	S13 flows in BCM/y	S14 flows in BCM/y	S15 flows in BCM/y
1	Lake_Victoria	24.0169	24.625	25.811	26.419	23.409	22.223	21.615
2	Nile_Victoria_Kyoga	24.0169	24.625	25.811	26.419	23.409	22.223	21.615
3	Lake_Kyoga	22.9359	23.559	24.606	25.229	22.312	21.266	20.642
4	Nile_Kyoga_Albert	22.9359	23.559	24.606	25.229	22.312	21.266	20.642
5	Lake_George	0	0.000	0.000	0.000	0.000	0.000	0.000
6	Kazinga_Channel	0	0.000	0.000	0.000	0.000	0.000	0.000
7	Lake_Edward	2.50008	2.750	2.500	2.750	2.250	2.500	2.250
8	River_Semliki	3.99608	4.246	4.146	4.396	3.746	3.846	3.596
9	Lake_Albert	26.89722	27.511	28.973	29.587	26.283	24.821	24.208
10	Albert_Nile	26.22479	26.823	28.249	28.847	25.626	24.201	23.602
11	Bahr_ElGebel_Nimule	30.24917	30.833	32.223	32.806	29.666	28.276	27.692
12	Bahr_El_Zaraf	7.56229	7.708	8.056	8.202	7.416	7.069	6.923
13	Bahr_ElGebel_Mongalla	7.56229	7.708	8.056	8.202	7.416	7.069	6.923
14	Bahr_El_Arab	0.5	0.500	0.500	0.500	0.500	0.500	0.500
15	Lake_No	8.06229	8.208	8.556	8.702	7.916	7.569	7.423
16	Sudd_Lake_No_Malakal	8.06229	8.208	8.556	8.702	7.916	7.569	7.423
17	River_Baro	9.23	9.230	9.230	9.230	9.230	9.230	9.230
18	River_Pibor	2.8	2.800	2.800	2.800	2.800	2.800	2.800
19	River_Sobat	13.53	13.530	13.530	13.530	13.530	13.530	13.530
20	Malakal	29.15459	29.446	30.141	30.433	28.863	28.168	27.876
21	White_Nile	24.11084	24.352	24.927	25.168	23.870	23.295	23.054
22	Gabal_Auliaa_Dam	24.11084	24.352	24.927	25.168	23.870	23.295	23.054
23	Nile_Auliaa_Khartoum	24.11084	24.352	24.927	25.168	23.870	23.295	23.054
24	Lake_Tana	3.801	3.801	3.801	3.801	3.801	3.801	3.801
25	Reach between Lake Tana and GERD	48.11604	48.116	48.116	48.116	48.116	48.116	48.116
26	GERD	48.11604	48.116	48.116	48.116	48.116	48.116	48.116
27	Reach between GERD and Rosaries Dam	48.11604	48.116	48.116	48.116	48.116	48.116	48.116
28	Rosaries Dam	48.11604	48.116	48.116	48.116	48.116	48.116	48.116
29	Reach between Rosaries and Sennar Dams	48.11604	48.116	48.116	48.116	48.116	48.116	48.116
30	Sennar Dam	48.11604	48.116	48.116	48.116	48.116	48.116	48.116
31	Between Sennar Dam and Khartoum	52.11604	52.116	52.116	52.116	52.116	52.116	52.116
32	Khartoum	76.22689	76.468	77.043	77.284	75.986	75.411	75.170
33	Reach between Khartoum and Atbara	76.22689	76.468	77.043	77.284	75.986	75.411	75.170
34	Upper Atbara	13.15561	13.156	13.156	13.156	13.156	13.156	13.156
35	Tekeze Dam	13.15561	13.156	13.156	13.156	13.156	13.156	13.156
36	Between Tekeze and Setit Dams	13.15561	13.156	13.156	13.156	13.156	13.156	13.156
37	Setit Dam	13.15561	13.156	13.156	13.156	13.156	13.156	13.156
38	Between Setit and Khashm El Girba Dams	13.15561	13.156	13.156	13.156	13.156	13.156	13.156
39	Khashm EL Girba Dam	13.15561	13.156	13.156	13.156	13.156	13.156	13.156
40	Between Khashm El Girba Dam and Atbara	13.15561	13.156	13.156	13.156	13.156	13.156	13.156
41	Atbara Confluence with Main Nile	89.3825	89.624	90.198	90.440	89.141	88.567	88.325
42	Between Atbara Confluence and Merowe Dam	89.3825	89.624	90.198	90.440	89.141	88.567	88.325
43	Merowe Dam	89.3825	89.624	90.198	90.440	89.141	88.567	88.325
44	Between Merowe Dam and Toshka	83.3825	83.624	84.198	84.440	83.141	82.567	82.325
45	Toshka Station	83.3825	83.624	84.198	84.440	83.141	82.567	82.325
46	Inlet to Toshka Depression	0	0.000	0.000	0.000	0.000	0.000	0.000
47	Toshka to Aswan Reach	83.3825	83.624	84.198	84.440	83.141	82.567	82.325
48	Lake Nasser	83.3825	83.624	84.198	84.440	83.141	82.567	82.325

S9 Base case; S10 Whilte Nile reaches areas increased by 10% (connected catchments not included); S11 Whilte Nile catchments areas increased by 10% (connected raeches not included); S12 Whilte Nile reaches and catchments areas increased 10%, S13 Whilte Nile reaches areas decreased by 10%; S14 Whilte Nile catchments areas decreased by 10%; S15 Whilte Nile reaches and catchments areas decreased 10%

DOI: 10.3844/ajessp.2025.49.78

Table 8: Effects of changes in land cover area on Flows at the Blue Nile Basin (Units 24-31)

Unit Number Figure (17)	Unit Name or Location	S9 Base case flows in BCM/y	S16 flows in BCM/y	S17 flows in BCM/y	S18 flows in BCM/y	S19 flows in BCM/y	S20 flows in BCM/y	S21 flows in BCM/y
1	Lake_Victoria	24.0169	24.017	24.017	24.017	24.017	24.017	24.017
2	Nile_Victoria_Kyoga	24.0169	24.017	24.017	24.017	24.017	24.017	24.017
3	Lake_Kyoga	22.9359	22.936	22.936	22.936	22.936	22.936	22.936
4	Nile_Kyoga_Albert	22.9359	22.936	22.936	22.936	22.936	22.936	22.936
5	Lake_George	0	0.000	0.000	0.000	0.000	0.000	0.000
6	Kazinga_Channel	0	0.000	0.000	0.000	0.000	0.000	0.000
7	Lake_Edward	2.50008	2.500	2.500	2.500	2.500	2.500	2.500
8	River_Semliki	3.99608	3.996	3.996	3.996	3.996	3.996	3.996
9	Lake_Albert	26.89722	26.897	26.897	26.897	26.897	26.897	26.897
10	Albert_Nile	26.22479	26.225	26.225	26.225	26.225	26.225	26.225
11	Bahr_ElGebel_Nimule	30.24917	30.249	30.249	30.249	30.249	30.249	30.249
12	Bahr_El_Zaraf	7.56229	7.562	7.562	7.562	7.562	7.562	7.562
13	Bahr_ElGebel_Mongalla	7.56229	7.562	7.562	7.562	7.562	7.562	7.562
14	Bahr_El_Arab	0.5	0.500	0.500	0.500	0.500	0.500	0.500
15	Lake_No	8.06229	8.062	8.062	8.062	8.062	8.062	8.062
16	Sudd_Lake_No_Malakal	8.06229	8.062	8.062	8.062	8.062	8.062	8.062
17	River_Baro	9.23	9.230	9.230	9.230	9.230	9.230	9.230
18	River_Pibor	2.8	2.800	2.800	2.800	2.800	2.800	2.800
19	River_Sobat	13.53	13.530	13.530	13.530	13.530	13.530	13.530
20	Malakal	29.15459	29.155	29.155	29.155	29.155	29.155	29.155
21	White_Nile	24.11084	24.111	24.111	24.111	24.111	24.111	24.111
22	Gabal_Auliaa_Dam	24.11084	24.111	24.111	24.111	24.111	24.111	24.111
23	Nile_Auliaa_Khartoum	24.11084	24.111	24.111	24.111	24.111	24.111	24.111
24	Lake_Tana	3.801	4.181	3.801	4.181	3.421	3.801	3.421
25	Reach between Lake Tana and GERD	48.11604	48.496	52.548	52.928	47.736	43.685	43.304
26	GERD	48.11604	48.496	52.548	52.928	47.736	43.685	43.304
27	Reach between GERD and Rosaries Dam	48.11604	48.496	52.548	52.928	47.736	43.685	43.304
28	Rosaries Dam	48.11604	48.496	52.548	52.928	47.736	43.685	43.304
29	Reach between Rosaries and Sennar Dams	48.11604	48.496	52.548	52.928	47.736	43.685	43.304
30	Sennar Dam	48.11604	48.496	52.548	52.928	47.736	43.685	43.304
31	Between Sennar Dam and Khartoum	52.11604	52.496	56.548	56.928	51.736	47.685	47.304
32	Khartoum	76.22689	76.607	80.658	81.038	75.847	71.795	71.415
33	Reach between Khartoum and Atbara	76.22689	76.607	80.658	81.038	75.847	71.795	71.415
34	Upper Atbara	13.15561	13.156	13.156	13.156	13.156	13.156	13.156
35	Tekeze Dam	13.15561	13.156	13.156	13.156	13.156	13.156	13.156
36	Between Tekeze and Setit Dams	13.15561	13.156	13.156	13.156	13.156	13.156	13.156
37	Setit Dam	13.15561	13.156	13.156	13.156	13.156	13.156	13.156
38	Between Setit and Khashm El Girba Dams	13.15561	13.156	13.156	13.156	13.156	13.156	13.156
39	Khashm EL Girba Dam	13.15561	13.156	13.156	13.156	13.156	13.156	13.156
40	Between Khashm El Girba Dam and Atbara	13.15561	13.156	13.156	13.156	13.156	13.156	13.156
41	Atbara Confluence with Main Nile	89.3825	89.763	93.814	94.194	89.002	84.951	84.571
42	Between Atbara Confluence and Merowe Dam	89.3825	89.763	93.814	94.194	89.002	84.951	84.571
43	Merowe Dam	89.3825	89.763	93.814	94.194	89.002	84.951	84.571
44	Between Merowe Dam and Toshka	83.3825	83.763	87.814	88.194	83.002	78.951	78.571
45	Toshka Station	83.3825	83.763	87.814	88.194	83.002	78.951	78.571
46	Inlet to Toshka Depression	0	0.000	0.000	0.000	0.000	0.000	0.000
47	Toshka to Aswan Reach	83.3825	83.763	87.814	88.194	83.002	78.951	78.571
48	Lake Nasser	83.3825	83.763	87.814	88.194	83.002	78.951	78.571

S9 Base case; S16 Blue Nile reaches areas increased by 10% (connected catchments not included); S17 Blue Nile catchments areas increased by 10% (connected raeches not included); S18 Blue Nile reaches and catchments areas increased 10%, S19 Blue Nile reaches areas decreased by 10%; S20 Blue Nile catchments areas decreased by 10%; S21 Blue Nile reaches and catchments areas decreased 10%

DOI: 10.3844/ajessp.2025.49.78

Table 9: Changes in Rainfall rates due to climate changes at the While Nile (units 1-23)

Unit Number Figure (17)	Unit Name or Location	S9 Base case flows in BCM/y	S22 flows in BCM/y	S23 flows in BCM/y	S24 flows in BCM/y	S25 flows in BCM/y	S26 flows in BCM/y	S27 flows in BCM/y
1	Lake_Victoria	24.0169	34.067	25.811	35.861	23.409	22.223	21.615
2	Nile_Victoria_Kyoga	24.0169	34.067	25.811	35.861	23.409	22.223	21.615
3	Lake_Kyoga	22.9359	33.213	24.606	34.883	22.312	21.266	20.642
4	Nile_Kyoga_Albert	22.9359	33.213	24.606	34.883	22.312	21.266	20.642
5	Lake_George	0	0.000	0.000	0.000	0.000	0.000	0.000
6	Kazinga_Channel	0	0.000	0.000	0.000	0.000	0.000	0.000
7	Lake_Edward	2.50008	2.750	2.500	2.750	2.250	2.500	2.250
8	River_Semliki	3.99608	4.246	4.146	4.396	3.746	3.846	3.596
9	Lake_Albert	26.89722	37.165	28.973	39.240	26.283	24.821	24.207
10	Albert_Nile	26.22479	36.235	28.249	38.259	25.626	24.201	23.602
11	Bahr_ElGebel_Nimule	30.24917	40.010	32.223	41.983	29.666	28.276	27.692
12	Bahr_El_Zaraf	7.56229	10.002	8.056	10.496	7.416	7.069	6.923
13	Bahr_ElGebel_Mongalla	7.56229	10.002	8.056	10.496	7.416	7.069	6.923
14	Bahr_El_Arab	0.5	0.500	0.500	0.500	0.500	0.500	0.500
15	Lake_No	8.06229	10.502	8.556	10.996	7.916	7.569	7.423
16	Sudd_Lake_No_Malakal	8.06229	10.502	8.556	10.996	7.916	7.569	7.423
17	River_Baro	9.23	9.230	9.230	9.230	9.230	9.230	9.230
18	River_Pibor	2.8	2.800	2.800	2.800	2.800	2.800	2.800
19	River_Sobat	13.53	13.530	13.530	13.530	13.530	13.530	13.530
20	Malakal	29.15459	34.035	30.141	35.021	28.863	28.168	27.876
21	White_Nile	24.11084	28.147	24.927	28.963	23.870	23.295	23.054
22	Gabal_Auliaa_Dam	24.11084	28.147	24.927	28.963	23.870	23.295	23.054
23	Nile_Auliaa_Khartoum	24.11084	28.147	24.927	28.963	23.870	23.295	23.054
24	Lake_Tana	3.801	3.801	3.801	3.801	3.801	3.801	3.801
25	Reach between Lake Tana and GERD	48.11604	48.116	48.116	48.116	48.116	48.116	48.116
26	GERD	48.11604	48.116	48.116	48.116	48.116	48.116	48.116
27	Reach between GERD and Rosaries Dam	48.11604	48.116	48.116	48.116	48.116	48.116	48.116
28	Rosaries Dam	48.11604	48.116	48.116	48.116	48.116	48.116	48.116
29	Reach between Rosaries and Sennar Dams	48.11604	48.116	48.116	48.116	48.116	48.116	48.116
30	Sennar Dam	48.11604	48.116	48.116	48.116	48.116	48.116	48.116
31	Between Sennar Dam and Khartoum	52.11604	52.116	52.116	52.116	52.116	52.116	52.116
32	Khartoum	76.22689	80.263	77.043	81.079	75.986	75.411	75.170
33	Reach between Khartoum and Atbara	76.22689	80.263	77.043	81.079	75.986	75.411	75.170
34	Upper Atbara	13.15561	13.156	13.156	13.156	13.156	13.156	13.156
35	Tekeze Dam	13.15561	13.156	13.156	13.156	13.156	13.156	13.156
36	Between Tekeze and Setit Dams	13.15561	13.156	13.156	13.156	13.156	13.156	13.156
37	Setit Dam	13.15561	13.156	13.156	13.156	13.156	13.156	13.156
38	Between Setit and Khashm El Girba Dams	13.15561	13.156	13.156	13.156	13.156	13.156	13.156
39	Khashm EL Girba Dam	13.15561	13.156	13.156	13.156	13.156	13.156	13.156
40	Between Khashm El Girba Dam and Atbara	13.15561	13.156	13.156	13.156	13.156	13.156	13.156
41	Atbara Confluence with Main Nile	89.3825	93.418	90.198	94.234	89.141	88.567	88.325
42	Between Atbara Confluence and Merowe Dam	89.3825	93.418	90.198	94.234	89.141	88.567	88.325
43	Merowe Dam	89.3825	93.418	90.198	94.234	89.141	88.567	88.325
44	Between Merowe Dam and Toshka	83.3825	87.418	84.198	88.234	83.141	82.567	82.325
45	Toshka Station	83.3825	87.418	84.198	88.234	83.141	82.567	82.325
46	Inlet to Toshka Depression	0	0.000	0.000	0.000	0.000	0.000	0.000
47	Toshka to Aswan Reach	83.3825	87.418	84.198	88.234	83.141	82.567	82.325
48	Lake Nasser	83.3825	87.418	84.198	88.234	83.141	82.567	82.325

S9 Base case; S22 Whilte Nile reaches rainfall increased by 10% (connected catchments not included); S23 Whilte Nile catchments rainfall increased by 10% (connected raeches not included); S24 Whilte Nile reaches and catchments rainfall increased 10%, S25 Whilte Nile reaches rainfall decreased by 10%; S26 Whilte Nile catchments rainfall decreased by 10%; S27 Whilte Nile reaches and catchments rainfall decreased 10%

DOI: 10.3844/ajessp.2025.49.78

Table 10: Changes in Rainfall rates due to climate changes at the Blue Nile (units 24-31)

Unit Number Figure (17)	Unit Name or Location	S9 Base case flows in BCM/y	S28 flows in BCM/y	S29 flows in BCM/y	S30 flows in BCM/y	S31 flows in BCM/y	S32 flows in BCM/y	S33 flows in BCM/y
1	Lake_Victoria	24.0169	24.017	24.017	24.017	24.017	24.017	24.017
2	Nile_Victoria_Kyoga	24.0169	24.017	24.017	24.017	24.017	24.017	24.017
3	Lake_Kyoga	22.9359	22.936	22.936	22.936	22.936	22.936	22.936
4	Nile_Kyoga_Albert	22.9359	22.936	22.936	22.936	22.936	22.936	22.936
5	Lake_George	0	0.000	0.000	0.000	0.000	0.000	0.000
6	Kazinga_Channel	0	0.000	0.000	0.000	0.000	0.000	0.000
7	Lake_Edward	2.50008	2.500	2.500	2.500	2.500	2.500	2.500
8	River_Semliki	3.99608	3.996	3.996	3.996	3.996	3.996	3.996
9	Lake_Albert	26.89722	26.897	26.897	26.897	26.897	26.897	26.897
10	Albert_Nile	26.22479	26.225	26.225	26.225	26.225	26.225	26.225
11	Bahr_ElGebel_Nimule	30.24917	30.249	30.249	30.249	30.249	30.249	30.249
12	Bahr_El_Zaraf	7.56229	7.562	7.562	7.562	7.562	7.562	7.562
13	Bahr_ElGebel_Mongalla	7.56229	7.562	7.562	7.562	7.562	7.562	7.562
14	Bahr_El_Arab	0.5	0.500	0.500	0.500	0.500	0.500	0.500
15	Lake_No	8.06229	8.062	8.062	8.062	8.062	8.062	8.062
16	Sudd_Lake_No_Malakal	8.06229	8.062	8.062	8.062	8.062	8.062	8.062
17	River_Baro	9.23	9.230	9.230	9.230	9.230	9.230	9.230
18	River_Pibor	2.8	2.800	2.800	2.800	2.800	2.800	2.800
19	River_Sobat	13.53	13.530	13.530	13.530	13.530	13.530	13.530
20	Malakal	29.15459	29.155	29.155	29.155	29.155	29.155	29.155
21	White_Nile	24.11084	24.111	24.111	24.111	24.111	24.111	24.111
22	Gabal_Auliaa_Dam	24.11084	24.111	24.111	24.111	24.111	24.111	24.111
23	Nile_Auliaa_Khartoum	24.11084	24.111	24.111	24.111	24.111	24.111	24.111
24	Lake_Tana	3.801	4.181	3.801	4.181	3.421	3.801	3.421
25	Reach between Lake Tana and GERD	48.11604	48.496	57.351	57.731	47.736	38.881	38.501
26	GERD	48.11604	48.496	57.351	57.731	47.736	38.881	38.501
27	Reach between GERD and Rosaries Dam	48.11604	48.496	57.351	57.731	47.736	38.881	38.501
28	Rosaries Dam	48.11604	48.496	57.351	57.731	47.736	38.881	38.501
29	Reach between Rosaries and Sennar Dams	48.11604	48.496	57.351	57.731	47.736	38.881	38.501
30	Sennar Dam	48.11604	48.496	57.351	57.731	47.736	38.881	38.501
31	Between Sennar Dam and Khartoum	52.11604	52.496	61.351	61.731	51.736	42.881	42.501
32	Khartoum	76.22689	76.607	85.462	85.842	75.847	66.992	66.612
33	Reach between Khartoum and Atbara	76.22689	76.607	85.462	85.842	75.847	66.992	66.612
34	Upper Atbara	13.15561	13.156	13.156	13.156	13.156	13.156	13.156
35	Tekeze Dam	13.15561	13.156	13.156	13.156	13.156	13.156	13.156
36	Between Tekeze and Setit Dams	13.15561	13.156	13.156	13.156	13.156	13.156	13.156
37	Setit Dam	13.15561	13.156	13.156	13.156	13.156	13.156	13.156
38	Between Setit and Khashm El Girba Dams	13.15561	13.156	13.156	13.156	13.156	13.156	13.156
39	Khashm EL Girba Dam	13.15561	13.156	13.156	13.156	13.156	13.156	13.156
40	Between Khashm El Girba Dam and Atbara	13.15561	13.156	13.156	13.156	13.156	13.156	13.156
41	Atbara Confluence with Main Nile	89.3825	89.763	98.617	98.997	89.002	80.148	79.768
42	Between Atbara Confluence and Merowe Dam	89.3825	89.763	98.617	98.997	89.002	80.148	79.768
43	Merowe Dam	89.3825	89.763	98.617	98.997	89.002	80.148	79.768
44	Between Merowe Dam and Toshka	83.3825	83.763	92.617	92.997	83.002	74.148	73.768
45	Toshka Station	83.3825	83.763	92.617	92.997	83.002	74.148	73.768
46	Inlet to Toshka Depression	0	0.000	0.000	0.000	0.000	0.000	0.000
47	Toshka to Aswan Reach	83.3825	83.763	92.617	92.997	83.002	74.148	73.768
48	Lake Nasser	83.3825	83.763	92.617	92.997	83.002	74.148	73.768

S9 Base case; S28 Blue Nile reaches rainfall increased by 10% (connected catchments not included); S29 Blue Nile catchments rainfall increased by 10% (connected raeches not included); S30 Blue Nile reaches and catchments rainfall increased 10%, S31 Blue Nile reaches rainfall decreased by 10%; S32 Blue Nile catchments rainfall decreased by 10%; S33 Blue Nile reaches and catchments rainfall decreased 10%

DOI: 10.3844/ajessp.2025.49.78

Table 11: Effects of changes in land use and dam operation on the Nile River Basin yield

Unit Number Figure (17)	Unit Name or Location	S9 Base case flows in BCM/y	S34 flows in BCM/y	S35 flows in BCM/y	S36 flows in BCM/y	S37 flows in BCM/y
1	Lake_Victoria	24.0169	15.047	24.017	15.047	24.017
2	Nile_Victoria_Kyoga	24.0169	15.047	24.017	15.047	24.017
3	Lake_Kyoga	22.9359	14.586	22.936	14.586	22.936
4	Nile_Kyoga_Albert	22.9359	14.586	22.936	14.586	22.936
5	Lake_George	0	0.000	0.000	0.000	0.000
6	Kazinga_Channel	0	0.000	0.000	0.000	0.000
7	Lake_Edward	2.50008	2.500	2.500	2.500	2.500
8	River_Semliki	3.99608	3.248	3.996	3.248	3.996
9	Lake_Albert	26.89722	16.518	26.897	16.518	26.897
10	Albert_Nile	26.22479	16.105	26.225	16.105	26.225
11	Bahr_ElGebel_Nimule	30.24917	20.382	30.249	20.382	30.249
12	Bahr_El_Zaraf	7.56229	5.096	7.562	5.096	7.562
13	Bahr_ElGebel_Mongalla	7.56229	5.096	7.562	5.096	7.562
14	Bahr_El_Arab	0.5	0.500	0.500	0.500	0.500
15	Lake_No	8.06229	5.596	8.062	5.596	8.062
16	Sudd_Lake_No_Malakal	8.06229	5.596	8.062	5.596	8.062
17	River_Baro	9.23	9.230	9.230	9.230	9.230
18	River_Pibor	2.8	2.800	2.800	2.800	2.800
19	River_Sobat	13.53	13.530	13.530	13.530	13.530
20	Malakal	29.15459	24.221	29.155	24.221	29.155
21	White_Nile	24.11084	20.031	24.111	20.031	24.111
22	Gabal_Auliaa_Dam	24.11084	20.031	24.111	20.031	24.111
23	Nile_Auliaa_Khartoum	24.11084	20.031	24.111	20.031	24.111
24	Lake_Tana	3.801	3.801	3.801	3.801	3.801
25	Reach between Lake Tana and GERD	48.11604	48.116	25.959	25.959	48.116
26	GERD	48.11604	48.116	25.959	25.959	28.116
27	Reach between GERD and Rosaries Dam	48.11604	48.116	25.959	25.959	28.116
28	Rosaries Dam	48.11604	48.116	25.959	25.959	28.116
29	Reach between Rosaries and Sennar Dams	48.11604	48.116	25.959	25.959	28.116
30	Sennar Dam	48.11604	48.116	25.959	25.959	28.116
31	Between Sennar Dam and Khartoum	52.11604	52.116	29.959	29.959	32.116
32	Khartoum	76.22689	72.147	54.069	49.989	56.227
33	Reach between Khartoum and Atbara	76.22689	72.147	54.069	49.989	56.227
34	Upper Atbara	13.15561	13.156	13.156	13.156	13.156
35	Tekeze Dam	13.15561	13.156	13.156	13.156	13.156
36	Between Tekeze and Setit Dams	13.15561	13.156	13.156	13.156	13.156
37	Setit Dam	13.15561	13.156	13.156	13.156	13.156
38	Between Setit and Khashm El Girba Dams	13.15561	13.156	13.156	13.156	13.156
39	Khashm El Girba Dam	13.15561	13.156	13.156	13.156	13.156
40	Between Khashm El Girba Dam and Atbara	13.15561	13.156	13.156	13.156	13.156
41	Atbara Confluence with Main Nile	89.3825	85.303	67.225	63.145	69.382
42	Between Atbara Confluence and Merowe Dam	89.3825	85.303	67.225	63.145	69.382
43	Merowe Dam	89.3825	85.303	67.225	63.145	69.382
44	Between Merowe Dam and Toshka	83.3825	79.303	61.225	57.145	63.382
45	Toshka Station	83.3825	79.303	61.225	57.145	63.382
46	Inlet to Toshka Depression	0	0.000	0.000	0.000	0.000
47	Toshka to Aswan Reach	83.3825	79.303	61.225	57.145	63.382
48	Lake Nasser	83.3825	79.303	61.225	57.145	63.382

S34 reduction of While Nile catchments' runoff coefficients by 50%; S35 reduction of Blue Nile catchments' runoff coefficients by 50%; S35 reduction of White and Blue Nile catchments' runoff coefficients by 50%; S37 storage of 20 BCM in GERD during average year

Case 6 has the same data as S3 except it has a precipitation p = 2.0 m/y which results in BNB yield at 71.9 BCM and Nile yield at Aswan = 107.2 BCM which are comparable to reporting by Mahmoud et al. (2022) of corresponding values of 1998-1999 high flood of 68.4 BCM and 107.04 BCM. It is also conforming with AbuZeid (2019) reporting that the Blue Nile flows during the period from year 1911-2015 shows a range from 20.69 BCM/y in year 1913-69.85 BCM/y in year 1929. Cases S5, S6 and S7 has the BNB yield as 31.5, 71.9 and 18.1 BCM/y, respectively which conform to the observed values.

Case S8, with a larger Blue Nile catchment, results in a higher Nile yield at Aswan (122 BCM), comparable to high flood events (Mahmoud et al. 2022). However, limited data for extreme events hinders accurate comparison with measured data.

The study compares its results with previous research findings. The predicted Blue Nile yield (48.116 BCM/year) and Main Nile yield at Aswan (83.3825 BCM/year) in Case S3 were close to the mean river natural flows reported by Sutcliffe and Parks (1999). The Blue Nile yield (39.8 BCM/year) in Case S4 was similar to the value based on satellite observations by Senay et al. (2009) with BNB of 41.4 BCM.

After conducting the River Basin Flow Model (RBFM) simulations for various real-world cases of rainfall, evaporation and loss rates and considering the existing river reaches and catchment areas, several scenarios were tested to assess potential changes in these variables. These scenarios, which assumed changes of ±10%, were designed to reflect alterations in land cover, rainfall patterns due to climate change and shifts in land use.

Land Cover Effects on Nile Water Yield

In these scenarios, land cover changes were simulated by adjusting the areas of the Nile River Basin units, including river reaches, lakes and their connected catchments. The White Nile units (units 1-23) and the Blue Nile units (units 24-31) were each increased and decreased by 10% to assess the impact on water yield. The analysis was carried out separately for river reaches and catchments, followed by a combined assessment.

For the White Nile, the results, as shown in Table (7), are compared to the base case (S9), where the Nile yields for the White Nile, Blue Nile and Lake Nasser were 24.11, 52.12 and 83.38 BCM, respectively. A 10% increase in the White Nile units led to water yield increases of 24.35 BCM (river reaches only), 24.93 BCM (catchments only) and 25.17 BCM (combined). These increases of 0.24, 0.82 and 1.06 BCM, respectively, are directly reflected in the flow at Aswan (unit 48). Conversely, a 10% decrease in the White Nile units resulted in corresponding yield decreases to 23.87, 23.30 and 23.05 BCM, with net reductions of 0.24, 0.82 and 1.06 BCM.

The maximum impact on the Nile flow occurred when both river reaches and catchments were altered together, underscoring the linearity of the flow balance equations. A key finding from this scenario is that a 10% increase or decrease in land cover area in the White Nile Basin roughly translates to a 1 BCM change in the Nile yield at Aswan.

For the Blue Nile Basin (units 24-31), Table (8) illustrates similar findings, with a 10% change in land cover area resulting in a more pronounced impact on the Nile yield. A 10% increase in land cover in the Blue Nile Basin generated an increase of about 5 BCM in water yield at Aswan, while a 10% decrease led to a reduction of the same magnitude. Notably, changes in catchment areas produced more significant effects than alterations in river reach areas. The Blue Nile, as expected, exhibits a higher sensitivity to land cover changes compared to the White Nile. Due to the model's linearity, the effects from both the White and Blue Nile can be combined to assess their cumulative impact on the Nile's water yield at Lake Nasser.

Climate Changes Effects on the Rainfall Rates with its signature on the Nile Water Yield:

To assess the impact of climate change, changes in rainfall rates were applied to the Nile Basin units. The assumption was made that soil infiltration had reached capacity, meaning that changes in runoff would directly correspond to changes in rainfall. Evapotranspiration losses were held constant, isolating the effect of rainfall variation on the Nile water flows.

Table (9) shows the results of rainfall changes in the White Nile Basin. A 10% increase in rainfall leads to a significant 4 BCM increase in White Nile yield. When considering all units river reaches, lakes and catchments —the yield increases by 5 BCM. Despite Lake Victoria receiving an increase of 10 BCM, this volume decreases as the water flows downstream due to losses along the river. In contrast, a 10% decrease in rainfall reduces the White Nile yield by approximately 1 BCM.

For the Blue Nile, Table (10) demonstrates that changes in rainfall have a far greater effect than in the White Nile. A 10% increase in rainfall in the Blue Nile Basin results in a nearly 10 BCM rise in water yield, while a 10% reduction causes a corresponding decrease of 10 BCM.

Effects of Land Use and Dam Operation on Nile Water Yield

Changes in land use, such as urbanization or agricultural expansion, can have dramatic effects on the Nile's water yield. Table (11) presents the results of a scenario in which runoff coefficients were reduced by 50%, leading to substantial reductions in Nile yield. In the White Nile, this reduction amounted to

approximately 4 BCM, while in the Blue Nile, it reached 22 BCM. When combined, the total reduction in Nile yield was around 26 BCM. These findings highlight the importance of land use changes on water resource availability, with the Blue Nile being particularly sensitive to such alterations.

Outside of the ongoing political discussions surrounding the Grand Ethiopian Renaissance Dam (GERD), a simple illustrative scenario is considered to highlight the potential hydrological impacts of water storage at GERD on downstream users. In this scenario, a storage volume of 20 BCM (billion cubic meters) is assumed to be retained in the dam during a typical average year. This hypothetical storage directly reduces the flow of water downstream, specifically from the Blue Nile Basin, by an equivalent volume of 20 BCM, as reflected in the model outputs summarized in Table (11).

The reduction in water yield from the Blue Nile Basin has significant implications for downstream users, particularly in Sudan and Egypt, where the Blue Nile is a critical contributor to the total Nile flow. The 20 BCM reduction not only affects water availability for agricultural irrigation, domestic consumption and industrial use but also has broader impacts on hydropower generation, navigation and ecosystem sustainability in these regions.

This simple run underscores the hydrological consequences of large-scale water storage in upstream reservoirs. While the scenario is limited in scope, it highlights the importance of carefully managing water resources to balance the needs of upstream development and downstream water security. The implications for downstream riparian nations depend on several factors, including the timing of storage, annual rainfall variability and the coordinated operation of existing downstream infrastructure such as the High Aswan Dam in Egypt.

Understanding these dynamics through modeling helps inform discussions and decisions on transboundary water management, emphasizing the need for cooperative solutions to manage shared water resources effectively.

Based on all of the above simulations, the study concludes that simple water balance models like RBFM can challenge complex models in the Nile Basin due to the lack of observed data. The lack of data hinders the development and evaluation of complex hydrological models in the region. The current study did not focus on specific flow conditions due to data limitations but rather presented scenarios that can reflect climate changes and changes in land cover and land use.

Conclusion

The Nile Basin, schematized in Figure (3) using 35 units, extends from Lake Victoria in the south to Lake Nasser in Egypt in the north. This representation, based on Abul-Atta's (1978) description, reflects conditions prevailing in the 1970s. Consequently, it does not include dams constructed after that period, such as GERD, Tekeze, Setit, Khasm El Girba and Merowe. However, it incorporates the Gebel-Aulia, Rosaries and Sennar Dams, which were operational at the time. The rainfall conditions correspond to average flood levels, resulting in an estimated water yield of approximately 84 BCM at Lake Nasser in Aswan, Egypt.

Multiple studies, including those by Abul-Atta (1978); Sutcliffe and Parks (1999); Ribbe and Ahmed (2006); Sayed (2008); AbuZeid (2019); Mahmoud et al. (2022), consistently report the total Nile Basin water resources as around 84 BCM/year of runoff measured at the Aswan High Dam.

Table (5) presents the flow calculations from the RBFM model for various units. Notably, the outflow at Lake Victoria is approximately 24 BCM, which remains consistent throughout the Equatorial lakes and Sudd regions, reaching the White Nile with the same volume. The Blue Nile yield at El-Diem station amounts to 50 BCM, contributing to a final Nile Basin yield of 84.112 BCM at Lake Nasser. The ratio of the Blue Nile Basin yield to the main Nile yield at Aswan (50/84.1 = 0.595) aligns with Abu-Zeid and Biswas's value of 0.6. The Rahad and Dinder tributaries are estimated to contribute an additional 4 BCM/year, bringing the total Blue Nile basin yield at Khartoum to 54 BCM/year.

For the Baro River reach (unit 17) before its confluence with the Pibor River, a flow of 13 BCM/year is used with a reach loss of 0.29, resulting in a net flow of 9.23 BCM/year. The Pibor River (unit 18) is assumed to have a flow of 2.8 BCM/year. Downstream of the confluence of the Baro and Pibor Rivers (unit 19), two tributary flows of 1.1 and 0.4 BCM/year are considered. The net flow for the Sobat River then becomes 9.23 + 2.8 + 0.4 + 1.1 = 13.53 BCM/year.

Lake Tana (unit 24) is characterized by a rainfall rate of 1.267 m/year and an area of 3000.0 km², yielding 3.8 BCM/year. Due to the lack of available data for tributaries in the reach between Lake Tana and GERD, eight point source tributary inflows, each with 5775 Million m3/year, are assumed, totaling 46.200 BCM/year. Adding this to the 3.8 BCM/year from Lake Tana, the total flow at the GERD location or El-Diem station becomes 50 BCM/year. The Upper Atbara River at the Tekeze dam (unit 34) has an inflow of 12 BCM/year, which flows through the entire Atbara River (unit 32) until it meets the main Nile at Atbara city.

Sutcliffe and Parks (1999) report mean river natural flows for the period ~1910 to 1995, as shown in Table (4): 16.1 BCM for the Sudd wetland at Malakal, 26.0 BCM for the White Nile at Khartoum, 48.3 BCM for the Blue Nile at Khartoum, 11.1 BCM at Atbara and 84.1 BCM for the main Nile River at Aswan. These values closely align with the corresponding RBFM model

results of mean annual flows: 15.6 BCM at Malakal (7.56 BCM from Bahr El Zaraf (unit 12) plus 8.06 BCM from Lake No (unit 16)), 24.1 BCM for the White Nile at Khartoum, 50 BCM for the Blue Nile at El Diem and 13.1 BCM for the Atbara River at Atbara. Wheeler et al. (2016) report the average annual flow at the GERD dam location (representing the water yield from the Blue Nile) as 49.4 BCM, while the RBFM model yields 50.001 BCM.

Mahmoud et al. (2022) indicate that the 1993–1994 hydrologic year corresponds to a normal natural flow of 84 BCM at the HAD. They further report annual flows at specific locations: (a) 75.34 BCM measured at the Dongola gauge; (b) 23.16 BCM released from Jabal Al Awlia; (c) 7.21 BCM measured at the Atbara River; and (d) 53.92 BCM (~ 54 BCM) measured at the El Diem gauge. They also report that the 1998–1999 hydrologic year represents a "high flood," with annual flows at specific locations: (a) 107.04 BCM measured at the Dongola gauge; (b) 28.23 BCM released from Jabal Al Awlia; (c) 17.76 BCM measured at the Atbara River; and (d) 68.40 BCM measured at the El Diem gauge.

Shahin (1998) reports that the peak discharge of the 1946 Nile flood at the Aswan gauge station was approximately 32,000 m^3/s, over 10 times the average annual Nile River discharge of around 2,800 m^3/s. This flood caused widespread devastation and damage along the river valley in Egypt, highlighting the immense power and variability of the Nile's seasonal flooding regime. This event was a key factor behind Egypt's decision to construct the High Aswan dam to mitigate the risks of such extreme floods. Understanding and mitigating the impacts of these floods remains a crucial challenge for the countries and communities along the Nile River. According to the National Oceanic and Atmospheric Administration (NOAA), the highest annual flood for the Nile River was recorded in 1964, with a discharge volume of approximately 62,000 m^3/s. This extraordinary flooding was caused by heavy rainfall in Ethiopia and Kenya. Unfortunately, complete data sets for rainfall, evaporation and seepage losses, among other factors, are not readily available to comprehensively test the developed model.

Now the study utilizes the River Basin Flow Model (RBFM) to simulate flow conditions in the Nile Basin, incorporating existing dams and exploring various hydrological scenarios. The model was applied to a schematization of the Nile Basin, representing the current state of the basin, including major dams like GERD, Tekeze, Setit, Khasm El Girba and Merowe in addition to Toshka intake as seen in Figure (17). The RBFM was run under different hydrological conditions, with varying input data for the Blue Nile and Atbara River. Lack of sufficient and accurate data for dam operations (especially GERD) and their associated hydrology prohibited their inclusion in detailed analyses and this is left for future studies.

The model uses a connected catchment area of 176,000 km^2 (cases S2 to S7) for the reach between Lake Tana and GERD (Unit 25), specified rainfall rates, losses due to evaporation and a runoff coefficient. For the Upper Atbara and Tekeze reach (Unit 34), the model uses a catchment area of 248,219.0 km^2, rainfall of 0.477 m/year, losses (evaporation) of 0.424 m/year and a runoff coefficient of 1.0, resulting in a flow discharge of 13.155 BCM/y routed through units 35 to 40 until it reaches the main Nile River at Atbara city.

The study explores eight different cases (S1 to S8) based on various data sources. Case S1 uses Abu-Atta 1978 data, similar to the results in Table 5. Case S2 is similar to S1 but with a Blue Nile catchment area of 176,000 km^2 (Conway 1997), while the precipitation (p) = 1.041 m/year, actual evapotranspiration (AET) = 0.781 m/year and C = 1.0 are according to Belete et al. (2018). Case S3 uses data representing maximum conditions according to Abera et al. (2017) with p = 1.59 m/year, AET = 0.827 m/year and C = 0.33. Case S4 employs average values reported by Abera et al. (2017) with p = 1.36 m/year, AET = 0.74 m/year and C = 0.33. Case S5 uses the lower limits of the data in Abera et al. (2017) with p = 1.13 m/year, AET = 0.653 m/year and C = 0.33. Case S6 is the same as S3 but with p = 2.0 m, representing a climate change scenario assuming heavy rain. Case S7 has p = 0.9 m/y, AET=0.653 m/y and C = 0.33, representing a climate change scenario assuming small rain. Case S8 is similar to case S2 but with a Blue Nile catchment area of 319,813 km^2 (Belete et al., 2018). The runoff coefficient was taken as 1.0 in the S2 and S8 cases as no reported data was found.

The results show varying Nile yields at Aswan, ranging from 53.4 BCM/year to 122 BCM/year. Cases 1 and 2 yield nearly identical results although the input data for the Blue Nile basin and Atbara are different which supports the validity of both of them. Case S3, using maximum conditions, predicts a Blue Nile yield of 48.116 BCM/y and a Main Nile yield at Aswan of 83.3825 BCM/y, closely resembling the mean river natural flows reported by Sutcliffe and Parks (1999). Case S4, using average conditions, produces a below-average yield, with a Blue Nile yield of 39.8 BCM/y and a Main Nile yield at Aswan of 75.08 BCM/y. Case S5 for the lower conditions yields BNB yield of 31.5 BCM/y and Nile yield at Aswan of 66.77 BCM/y. Abera et al. (2017) using the JGrass-NewAge model system and satellite data obtained runoff yield from the Blue Nile Basin of 0.614, 0.454 and 0.294 m/y for the maximum, average and minimum conditions. Using BNB area of 176,000 km^3, these values correspond to yield of 108.1, 79.9 and 51.7 BCM/y versus corresponding values of the RBFM of 48.1, 39.8 and 31.5 BCM/y. The above values by Abera et al. (2017) seem to be high as according to AbuZeid (2019) the Blue Nile flows during the period from year 1911 to 2015 (105 years of records) shows a range from 20.69 BCM/y in year 1913 to 69.85 BCM/y in year 1929.

Case 6 has the same data as S3 except it has a precipitation p = 2.0 m/y which results in BNB yield at 71.9 BCM and Nile yield at Aswan = 107.2 BCM which are comparable to reporting by Mahmoud et al. (2022) of corresponding values of 1998-1999 high flood of 68.4 BCM and 107.04 BCM. It is also conforming with AbuZeid (2019) reporting that the Blue Nile flows during the period from year 1911 to 2015 shows a range from 20.69 BCM/y in year 1913 to 69.85 BCM/y in year 1929. Cases S5, S6 and S7 has the BNB yield as 31.5, 71.9 and 18.1 BCM/y, respectively which conform to the observed values.

Case S8, with a larger Blue Nile catchment, results in a higher Nile yield at Aswan (122 BCM), comparable to high flood events (Mahmoud et al. 2022). However, limited data for extreme events hinders accurate comparison with measured data.

The study compares its results with previous research findings. The predicted Blue Nile yield (48.116 BCM/year) and Main Nile yield at Aswan (83.3825 BCM/year) in Case S3 were close to the mean river natural flows reported by Sutcliffe and Parks (1999). The Blue Nile yield (39.8 BCM/year) in Case S4 was similar to the value based on satellite observations by Senay et al. (2009) with BNB of 41.4 BCM.

After conducting the River Basin Flow Model (RBFM) simulations for various real-world cases of rainfall, evaporation and loss rates and considering the existing river reaches and catchment areas, several scenarios were tested to assess potential changes in these variables. These scenarios, which assumed changes of ±10%, were designed to reflect alterations in land cover, rainfall patterns due to climate change and shifts in land use.

Land Cover Effects on Nile Water Yield

In these scenarios, land cover changes were simulated by adjusting the areas of the Nile River Basin units, including river reaches, lakes and their connected catchments. The White Nile units (units 1-23) and the Blue Nile units (units 24-31) were each increased and decreased by 10% to assess the impact on water yield. The analysis was carried out separately for river reaches and catchments, followed by a combined assessment.

For the White Nile, the results, as shown in Table (7), are compared to the base case (S9), where the Nile yields for the White Nile, Blue Nile and Lake Nasser were 24.11, 52.12 and 83.38 BCM, respectively. A 10% increase in the White Nile units led to water yield increases of 24.35 BCM (river reaches only), 24.93 BCM (catchments only) and 25.17 BCM (combined). These increases of 0.24, 0.82 and 1.06 BCM, respectively, are directly reflected in the flow at Aswan (unit 48). Conversely, a 10% decrease in the White Nile units resulted in corresponding yield decreases to 23.87, 23.30 and 23.05 BCM, with net reductions of 0.24, 0.82 and 1.06 BCM.

The maximum impact on the Nile flow occurred when both river reaches and catchments were altered together, underscoring the linearity of the flow balance equations. A key finding from this scenario is that a 10% increase or decrease in land cover area in the White Nile Basin roughly translates to a 1 BCM change in the Nile yield at Aswan.

For the Blue Nile Basin (units 24 to 31), Table (8) illustrates similar findings, with a 10% change in land cover area resulting in a more pronounced impact on the Nile yield. A 10% increase in land cover in the Blue Nile Basin generated an increase of about 5 BCM in water yield at Aswan, while a 10% decrease led to a reduction of the same magnitude. Notably, changes in catchment areas produced more significant effects than alterations in river reach areas. The Blue Nile, as expected, exhibits a higher sensitivity to land cover changes compared to the White Nile. Due to the model's linearity, the effects from both the White and Blue Nile can be combined to assess their cumulative impact on the Nile's water yield at Lake Nasser.

Climate Changes Effects on the Rainfall Rates with its signature on the Nile Water Yield:

To assess the impact of climate change, changes in rainfall rates were applied to the Nile Basin units. The assumption was made that soil infiltration had reached capacity, meaning that changes in runoff would directly correspond to changes in rainfall. Evapotranspiration losses were held constant, isolating the effect of rainfall variation on the Nile water flows.

Table (9) shows the results of rainfall changes in the White Nile Basin. A 10% increase in rainfall leads to a significant 4 BCM increase in White Nile yield. When considering all units—river reaches, lakes and catchments—the yield increases by 5 BCM. Despite Lake Victoria receiving an increase of 10 BCM, this volume decreases as the water flows downstream due to losses along the river. In contrast, a 10% decrease in rainfall reduces the White Nile yield by approximately 1 BCM.

For the Blue Nile, Table (10) demonstrates that changes in rainfall have a far greater effect than in the White Nile. A 10% increase in rainfall in the Blue Nile Basin results in a nearly 10 BCM rise in water yield, while a 10% reduction causes a corresponding decrease of 10 BCM.

Effects of Land Use and Dam Operation on Nile Water Yield

Changes in land use, such as urbanization or agricultural expansion, can have dramatic effects on the Nile's water yield. Table (11) presents the results of a scenario in which runoff coefficients were reduced by 50%, leading to substantial reductions in Nile yield. In the White Nile, this reduction amounted to

approximately 4 BCM, while in the Blue Nile, it reached 22 BCM. When combined, the total reduction in Nile yield was around 26 BCM. These findings highlight the importance of land use changes on water resource availability, with the Blue Nile being particularly sensitive to such alterations.

Outside of the ongoing political discussions surrounding the Grand Ethiopian Renaissance Dam (GERD), a simple illustrative scenario is considered to highlight the potential hydrological impacts of water storage at GERD on downstream users. In this scenario, a storage volume of 20 BCM (billion cubic meters) is assumed to be retained in the dam during a typical average year. This hypothetical storage directly reduces the flow of water downstream, specifically from the Blue Nile Basin, by an equivalent volume of 20 BCM, as reflected in the model outputs summarized in Table (11).

The reduction in water yield from the Blue Nile Basin has significant implications for downstream users, particularly in Sudan and Egypt, where the Blue Nile is a critical contributor to the total Nile flow. The 20 BCM reduction not only affects water availability for agricultural irrigation, domestic consumption and industrial use but also has broader impacts on hydropower generation, navigation and ecosystem sustainability in these regions.

This simple run underscores the hydrological consequences of large-scale water storage in upstream reservoirs. While the scenario is limited in scope, it highlights the importance of carefully managing water resources to balance the needs of upstream development and downstream water security. The implications for downstream riparian nations depend on several factors, including the timing of storage, annual rainfall variability and the coordinated operation of existing downstream infrastructure such as the High Aswan Dam in Egypt.

Understanding these dynamics through modeling helps inform discussions and decisions on transboundary water management, emphasizing the need for cooperative solutions to manage shared water resources effectively.

Based on all of the above simulations, the study concludes that simple water balance models like RBFM can challenge complex models in the Nile Basin due to the lack of observed data. The lack of data hinders the development and evaluation of complex hydrological models in the region. The current study did not focus on specific flow conditions due to data limitations but rather presented scenarios that can reflect climate changes and changes in land cover and land use.

Acknowledgment

The author would like to present his sincere gratitude and appreciation to anonymous reviewers for the very fruitful, informative and important remarks, suggestions and comments which really helped in the significant improving of this manuscript.

Funding Information

This study has not received any funding.

Author's Contributions

The author independently carried out all aspects of this study, including the comprehensive literature review, conceptualization of the model, its development and implementation, as well as the preparation, drafting, refinement and final writing of the manuscript. Additionally, the author conducted a thorough review and editing process to ensure the quality and coherence of the final document.

Ethics

The author declares that he has no known competing financial interests or personal relationships that could have appeared to influence the work reported in this study and that this study adheres to ethics.

References

Abd-El Moneim, H., Soliman, M. R., & Moghazy, H. M. (2017). Numerical simulation of Blue Nile Basin using distributed hydrological model. *11th International Conference on the Role of Engineering towards a Better Environment (RETBE'17)*, 8-20.

Abdel-Aziz, O. R. (2014). Flood forecasting in Blue Nile basin using a process-based hydrological model. *International Journal of Environment*, *3*(1), 10-21. https://doi.org/10.3126/ije.v3i1.9938

Abera, W., Formetta, G., Brocca, L., & Rigon, R. (2017). Modeling the water budget of the Upper Blue Nile basin using the JGrass-NewAge model system and satellite data. *Hydrology and Earth System Sciences*, *21*(6), 3145-3165. https://doi.org/10.5194/hess-21-3145-2017

Abul-Atta, A. A. (1978). *Egypt and the Nile after the construction of the High Aswan Dam*.

AbuZeid, K. M. (2019). Potential Hydrological Impacts of the Grand Ethiopian Renaissance Dam on Egypt and Sudan. *Arab Water Council Journal*, *10*(2), 1.

AbuZeid, K. M. (2021). Potential Transboundary Impacts of the Grand Ethiopian Renaissance Dam Under Climate Change and Variability. *Climate Change and Water Resources in Africa: Perspectives and Solutions Towards an Imminent Water Crisis*, 359-386. https://doi.org/10.1007/978-3-030-61225-2_16

Abu-Zeid, M. A., & Biswas, A. K. (1996). *River basin planning and management*. Oxford University Press.

Ahmed, M., Abdelrehim, R., Elshalkany , M., & Abdrabou, M. (2024). Impacts of the Grand Ethiopian Renaissance Dam on the Nile River's downstream reservoirs. *Journal of Hydrology*, *633*, 130952-130952. https://doi.org/10.1016/j.jhydrol.2024.130952

Awulachew, S. B., McCartney, M., Steenhuis, T. S., & Ahmed, A. A. (2009). *A Review of Hydrology, Sediment and Water Resource Use in the Blue Nile Basin*.

Bashar, K. E., Mutua, F., Mulungu, D. M., Deksyos, T., & Shamseldin, A. Y. (2005). Appraisal study to select suitable Rainfall-Runoff model(s) for the Nile River Basin. *Proceedings of International Conference of UNESCO Flanders Fust Friend/Nile Project*. Proceedings of International Conference of UNESCO Flanders Fust Friend/Nile Project.

Belete, M., Deng, J., Zhou, M., Wang, K., You, S., Hong, Y., & Weston, M. (2018). A New Approach to Modeling Water Balance in Nile River Basin, Africa. *Sustainability*, *10*(3), 810. https://doi.org/10.3390/su10030810

Conway, D. (1997). A water balance model of the Upper Blue Nile in Ethiopia. *Hydrological Sciences Journal*, *42*(2), 265-286. https://doi.org/10.1080/02626669709492024

Conway, D. (2000). The Climate and Hydrology of the Upper Blue Nile River. *The Geographical Journal*, *166*(1), 49-62. https://doi.org/10.1111/j.1475-4959.2000.tb00006.x

DaWen, Y., Oki, T., Herath, S., & Musiake, K. (2002). A geomorphology-based hydrological model and its applications. *Mathematical Models of Small Watershed Hydrology and Applications*, *9*, 259-300.

Digna, R. F., Mohamed, Y. A., Zaag, P. van der, Uhlenbrook, S., Krogt, Wil van der, & Corzo, G. (2018). Impact of Water Resources Development on Water Availability for Hydropower Production and Irrigated Agriculture of the Eastern Nile Basin. *Journal of Water Resources Planning and Management*, *144*(5), 05018007. https://doi.org/10.1061/(ASCE)WR.1943-5452.0000912

Eldeeb, H., Mowafy, M. H., Salem, M. N., & Ibrahim, A. (2023). Flood propagation modeling: Case study the Grand Ethiopian Renaissance dam failure. *Alexandria Engineering Journal*, *71*, 227-237. https://doi.org/10.1016/j.aej.2023.03.054

Hassan, M. A., Hassan, M. F., Mohamed, Y. A., & Awad, W. A. (2023). Dam operation using satellite data and hydrological models: the case of Roseires dam and Grand Ethiopian Renaissance Dam in the Blue Nile River. *Water International*, *48*(8), 975-999. https://doi.org/10.1080/02508060.2023.2286412

Heggy, E., Sharkawy, Z., & Abotalib, A. Z. (2021). Egypt's water budget deficit and suggested mitigation policies for the Grand Ethiopian Renaissance Dam filling scenarios, Environ. *Environmental Research Letters*, *16*, 074022. https://doi.org/10.1088/1748-9326/ac0ac9

Kamel, A. M., Amin, D. M., & Nour Eldin, M. M. N. (2019a). Assessment the harm from the Grand Ethiopian Renaissance Dam on the water inflow to Egypt. *International Research Journal of Engineering and Technology (IRJET)*, *6*(10), 218-225.

Kamel, A. M., Amin, D., & Nour Eldin, M. M. N. (2019b). Updating and Assessment of the Eastern Nile Model in RiverWare for Reservoir Management. *International Journal of Applied Engineering Research*, *14*(8), 1772-1781.

Kojiri, T., Tokai, A., & Kinai, Y. (1998). Assessment of river basin environment though simulation with water quality and quantity. *Kyoto University*, *41*, 119-134.

Lenderink, G., Hurk, B., Meigaard, E., Ulden, A., & Cuijpers, H. (2003). *Simulation of present-day climate in RACMO2: first results and model developments*.

Lorenz, C., Portele, T. C., Shrestha, P., Hassan, M. A., Osman, M., Samaniego, L., Laux, P., & Kunstmann, H. (2019). Regionalized global and seasonal information for the transboundary water management: Examples from the Tekeze-Atbara and Blue Nile basins [Paper presentation]. *Tekeze-Atbara Basin Conference on Water Related Studies at: Khartoum*. Tekeze-Atbara basin conference on water related studies at: Khartoum, Sudan.

Mahmoud, M. R., Fahmy, Hussam, & Garcia, L. A. (2022). Potential impacts of failure of the Grand Ethiopian Renaissance Dam on downstream countries. *Journal of Flood Risk Management*, *15*(2), e12793. https://doi.org/10.1111/jfr3.12793

Manning, J. C. (1997). *Applied Principles of Hydrology*.

Mohamed, Y. A., van den Hurk, B. J. J. M., Savenije, H. H. G., & Bastiaanssen, W. G. M. (2005). Hydroclimatology of the Nile: results from a regional climate model. *Hydrology and Earth System Sciences*, *9*(3), 263-278. https://doi.org/10.5194/hess-9-263-2005

Nile Forecast System. (2012). *Improvement of the Nile Forecast System (NFS)*.

Ribbe, L., & Ahmed, S. (2006). Transboundary Water Management in the Nile River Basin". *Technology, Resource Management and Development*, 13-26.

Samaniego, L., Kumar, R., & Jackisch, C. (2011). Predictions in a data-sparse region using a regionalized grid-based hydrologic model driven by remotely sensed data. *Hydrology Research*, *42*(5), 338-355. https://doi.org/10.2166/nh.2011.156

Sayed, M. A. A. (2008). Eastern Nile Planning Model, Integration with IDEN Projects to Deal with Climate Change Uncertainty and Flooding Risk. *Nile Water Science & Engineering Journal*, *1*(1), 86-93.

Senay, G. B., Asante, K., & Artan, G. (2009). Water balance dynamics in the Nile Basin. *Hydrological Processes*, *23*(26), 3675-3681. https://doi.org/10.1002/hyp.7364

Shahin, M. (1998). Development of flood events and their magnitudes on the Nile River. *Hydrological Sciences Journal*, *43*(3), 337-349.

Sutcliffe, J. V., & Parks, Y. P. (1999). *The Hydrology of the Nile*.

van Dam, J. C., Wosten, J. H. M., & Nemas, A. (2000). Unsaturated soil water movement in hysteretic and water repellent field soils. *Journal of Hydrology*, *184*(3/4), 153-173. https://doi.org/10.1016/0022-1694(95)02996-6

Wheeler, K. G., Basheer, M., Mekonnen, Z. T., Eltoum, S. O., Mersha, A., Abdo, G. M., Zagona, E. A., Hall, J. W., & Dadson, S. J. (2016). Cooperative filling approaches for the Grand Ethiopian Renaissance Dam. *Water International*, *41*(4), 611-634,. https://doi.org/10.1080/02508060.2016.1177698

Wheeler, K. G., & Setzer, S. (2012). *Eastern Nile River Ware planning model*.